Ciencia y Tecnología
Secretaría de Ciencia, Humanidades, Tecnología e Innovación

Galaxies

Itziar Aretxaga (itziar@inaoep.mx)
INAOE, Mexico
46 ISYA, Ecuador, July 2025

Lecture 1: Introduction to the galaxy zoo:

- Galaxy types and classification schemes
- General properties and structure
- Standard stellar population indicators
- Cold/Warm gas in galaxies
- Dust in galaxies
- Dark matter in galaxies

Bibliography and important references:

- Ned Wright´s Cosmology Calculator: http://www.astro.ucla.edu/~wright/CosmoCalc.html
- NASA Extragalactic Database: http://ned.ipac.caltech.edu
- Papers in ADS referenced throughout the notes
- Extragalactic Astronomy and Cosmology (2015), Peter Schneider, Springer.
- Mo, van den Bosch & White (2010). Galaxy Formation and Evolution, CUP.
- Galaxies in the Universe, Sparke & Gallagger, (2007), Cambridge University Press

(Acknowledgements to Pablo Pérez González and Rafael Guzmán for their lecture notes)

Galaxy

A galaxy is a self-gravitating assemble of stars, gas, dust and dark matter (DM) that constitutes the fundamental building block to trace structure in the Universe.

The word galaxy is derived from the Greek galaxias (γαλαξίας), literally "milky", a reference to the Milky Way.

They have typical masses $M \sim 10^9$ -10^{13} $M_\odot$

The Milky Way is the galaxy that contains our Solar System: $M^* \sim 6x\ 10^{10}\ M_\odot$, $M_{vir} \sim 10^{12}\ M_\odot$, diameter ~31-55 kpc, thickness of disk ~ 0.6 kpc, Sun´s distance to galactic center ~ 8.5 kpc

(pc= $3.08567758 \times 10^{16}$ m, $M_\odot = 1.9891 \times 10^{30}$ kilograms)

There are many acronyms for classes of galaxies under different selection criteria and classification schemes:

E, Sb, Sa, Sab, S0, E, SBa,Sba(r), Irr, Im, cD, SB, LAE, LBG,SMG, LIRG, ULIRG, ERO, BzK, LSBG, AGN, …

Structure of Milky Way

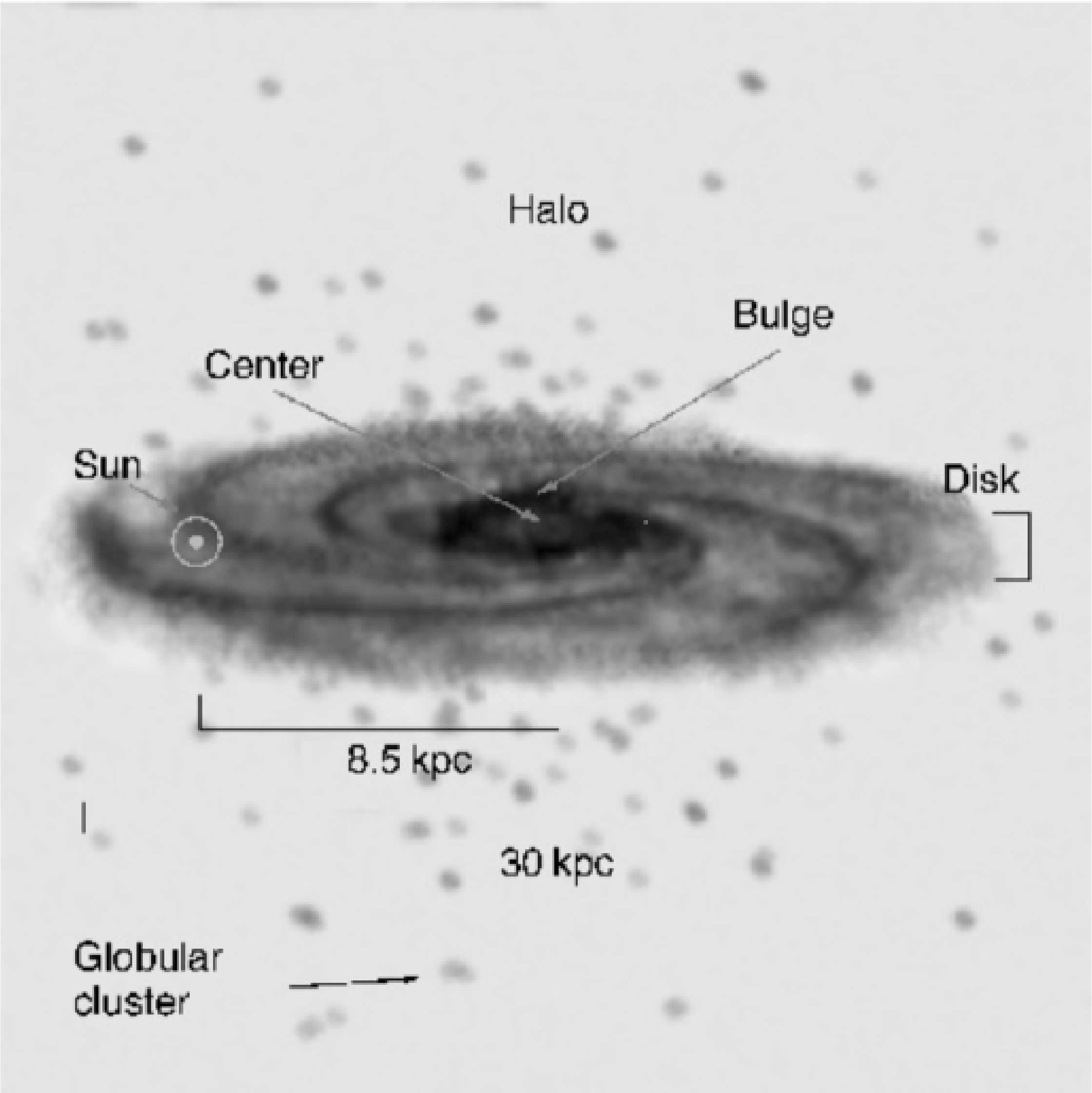

Our local group of galaxies

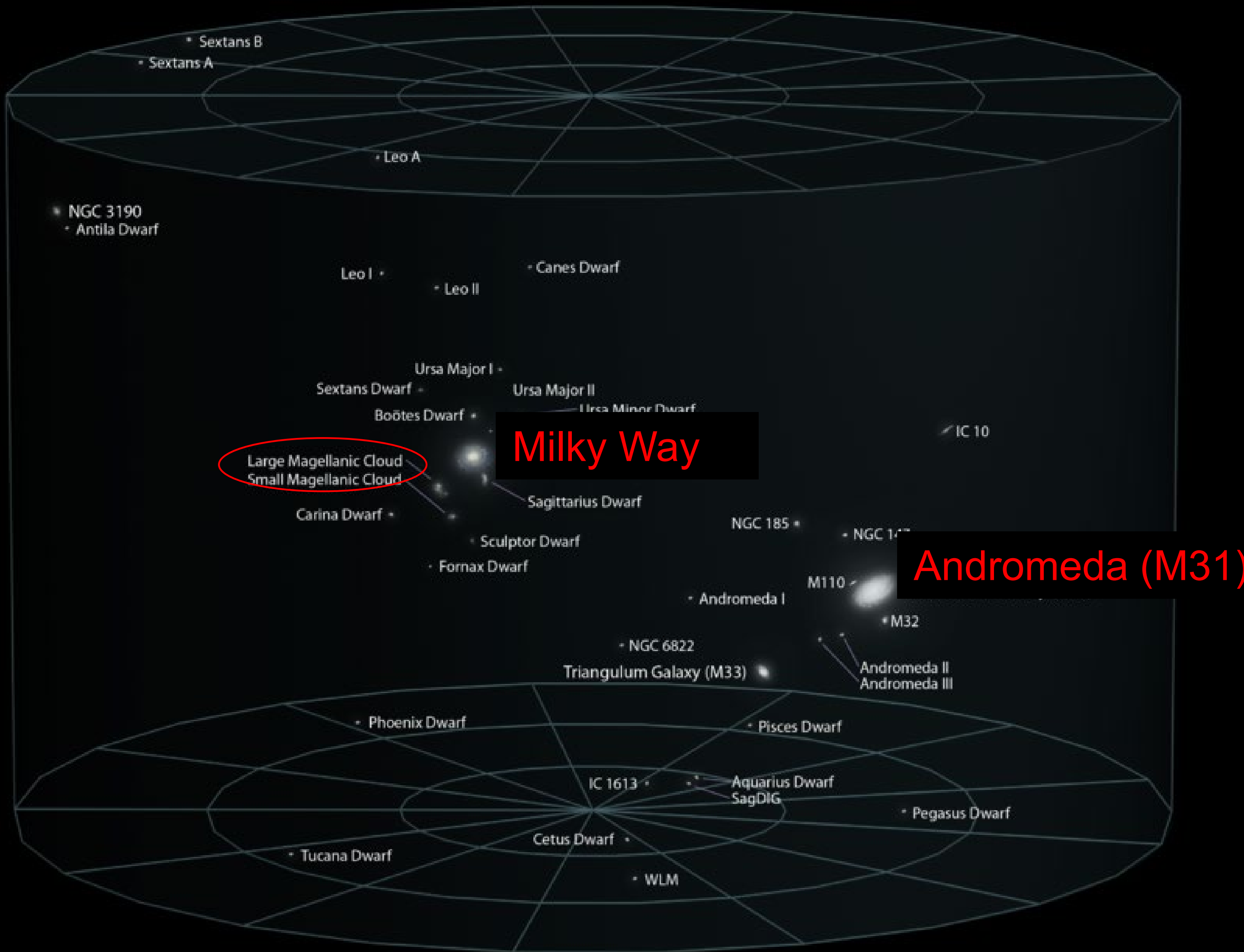

Our local group of galaxies

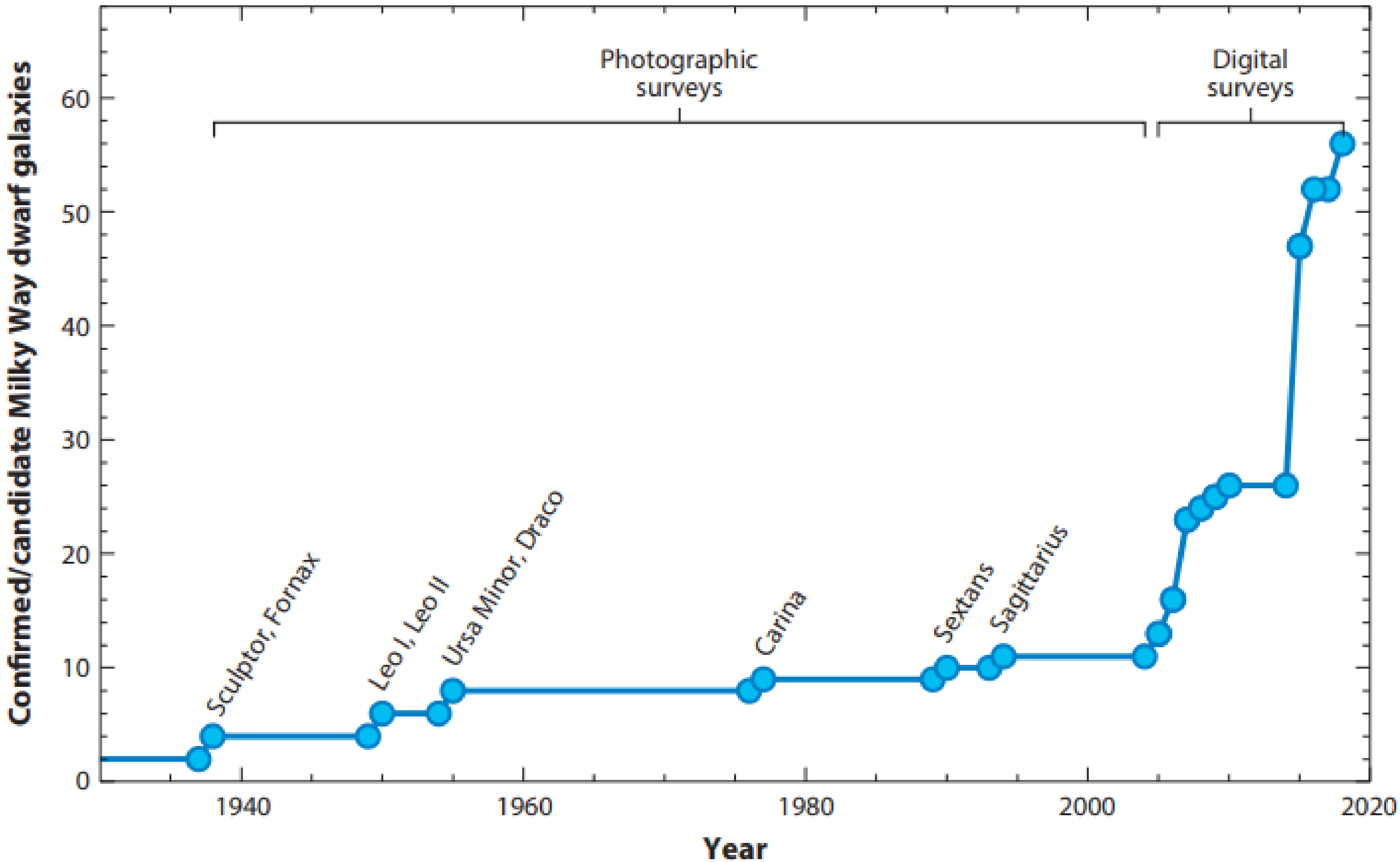

Figure 1

Census of Milky Way satellite galaxies as a function of time. The objects shown here include all spectroscopically confirmed dwarf galaxies as well as those suspected to be dwarfs based on less conclusive spectroscopic and photometric measurements. The major discovery impact of the Sloan Digital Sky Survey (SDSS; from 2005–2010), the Dark Energy Survey (DES), and the Panoramic Survey Telescope & Rapid Response System (Pan-STARRS; 2015), each of which approximately doubled the previously known satellite population, stands out in this historical perspective.

(Simon 2019 ARAA)

The discovery of galaxies

- 1755 Immanuel Kant: nebulae are independent systems made of stars
- 1771 Messier´s Catalogue «*Catalogue des Nébuleuses et des amas d'Étoiles, que l'on découvre parmi les Étoiles fixes sur l'horizon de Paris*» M31 (Andromeda), M33 (Triangulum), M82, M87,… M103
- 1786 William Herschel´s “Catalogue of Nebulae and Clusters of Stars” to be later expanded into the “General Catalogue of Nebulae and Clusters of Stars” (GC) by John Herschel. The CN and GC are the precursors to John Louis Emil Dreyer's “New General Catalogue” (NGC): NGC4151, NGC5548, …

- 1868 William Huggings’ M31 spectrum: flat unlike others (planetary nebulae)
- 1885 William Parson, 3rd Earl of Rosse, with his 72-inch speculum-metal reflector: spiral structures in M33, M51, M101
- 1890 Keeler & Curtis, 36" at Lick Observatory and photography: spirals common
- 1908 Henrietta Swan Leavitt´s L-P Cepheid correlation in *Annals of the Astronomical Observatory of Harvard College*
- 1912 V. Slipher´s spectra at Lowell Obs., M31 large radial velocity
- 1917: Herber Curtis nobas in M31 hence M31 at great distance

The discovery of galaxies

- 1920: Sharpley-Curtis Great Debate -> start of Extragalactic Astronomy, galaxies are “island universes” outside the Milky Way (https://apod.nasa.gov/debate/1920/cs_nrc.html)
  - The “white nebulae" occur far from the galactic plane, in fact avoiding it, unlike other nebular constituents
  - Some galaxies, seen edge-on, look much like the visual Milky Way

- 1925-29: Edwin Hubble identifies Cepheid stars in M31, M33 and IC1613 - > precision distances using Leavitt´s law, or L-P method

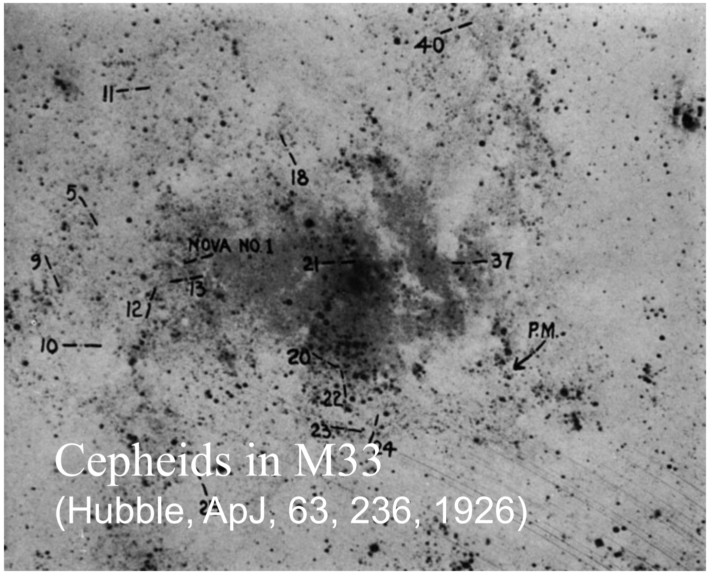

Cepheids in M33
(Hubble, ApJ, 63, 236, 1926)

Photometric systems in the optical-IR

Aparent magnitude

$$m_\lambda = -2.5\log f_\lambda + C_\lambda$$
$$= -2.5\log L_\lambda/4\pi d^2 + C_\lambda$$

$$C_\lambda = 2.5\log f_\lambda(0)$$

Absolute magnitude

$$M_\lambda = -2.5\log L_\lambda/4\pi(10pc)^2 + C_\lambda$$

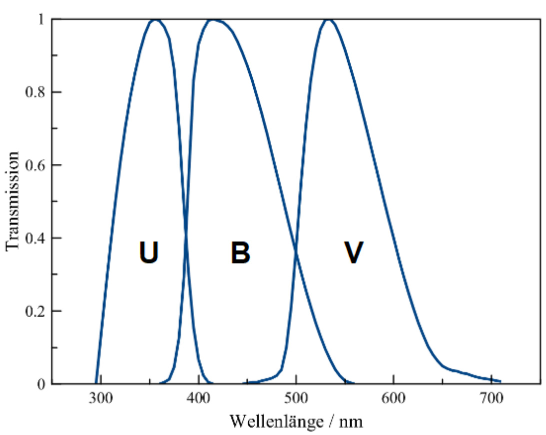

Standard photometric systems

Standard U, B, V, R, I and long wavelength systems

Filter band	λ_0[a] (μm)	$\Delta\lambda_0$ (FWHM) (μm)	Absolute spectral irradiance for mag = 0.0: $f_\lambda(0)$ (erg cm^{-2} s^{-1} Å^{-1})	$f_\nu(0)$ (W m^{-2} Hz^{-1})
U	0.365	0.068	4.27×10^{-9}	1.90×10^{-23}
B	0.44	0.098	6.61×10^{-9}	$4.27(4.64)$[b] $\times10^{-23}$
V	0.55	0.089	3.64×10^{-9}	3.67×10^{-23}
R	0.70	0.22	1.74×10^{-9}	2.84×10^{-23}
I	0.90	0.24	8.32×10^{-10}	2.25×10^{-23}
J	1.25	0.3	3.18×10^{-10}	1.65×10^{-23}
H	1.65	0.4	1.18×10^{-10}	1.07×10^{-23}
K	2.2	0.6	4.17×10^{-11}	6.73×10^{-24}
L	3.6	1.2	6.23×10^{-12}	2.69×10^{-24}
M	4.8	0.8	2.07×10^{-12}	1.58×10^{-24}
N	10.2		1.23×10^{-13}	4.26×10^{-25}

[a] $\lambda_0 = \int \lambda S(\lambda)\,d\lambda / \int S(\lambda)\,d\lambda$, where $S(\lambda)$ is the photometer response function.
[b] From S. Kleinmann.
U, B, R, I, N values from Allen, C. W., *Astrophysical Quantities*. The Athlone Press (1973). *V, J, H, K, L, M* values from Wamsteker, W., *Astron. Astrophys.*, **97**, 329 (1981).

The spectral irradiance for a star of a given magnitude is given either by:

$$\log f_\lambda(m_x) = -0.4m_x + \log f_\lambda(0),$$

where $f_\lambda(m_x)$ is the spectral irradiance in erg cm^{-2} s^{-1} Å^{-1} of a star of magnitude (m_x) in the x filter band at the mean wavelength $\lambda_0(x)$, or

$$\log f_\nu(m_x) = -0.4m_x + \log f_\nu(0),$$

where $f_\nu(m_x)$ is the spectral irradiance in W m^{-2} Hz^{-1}.

Primary distance indicators: Cepheids (<20 Mpc)

Cepheid stars are long-period variables (~1-100 days) and they display a tight luminosity-period linear relationship (better than 10% precision), which is weakly dependent on metallicity.

$$\boxed{M_V = -2.80 \log P_{\mathrm{d}} - (1.43 \pm 0.1)}$$ (Feast & Catchpole 1997)

$$\boxed{\delta(m - M)_0 = -0.24 \pm 0.16}$$ (Kennicut et al. 1998) Metal rich brighter

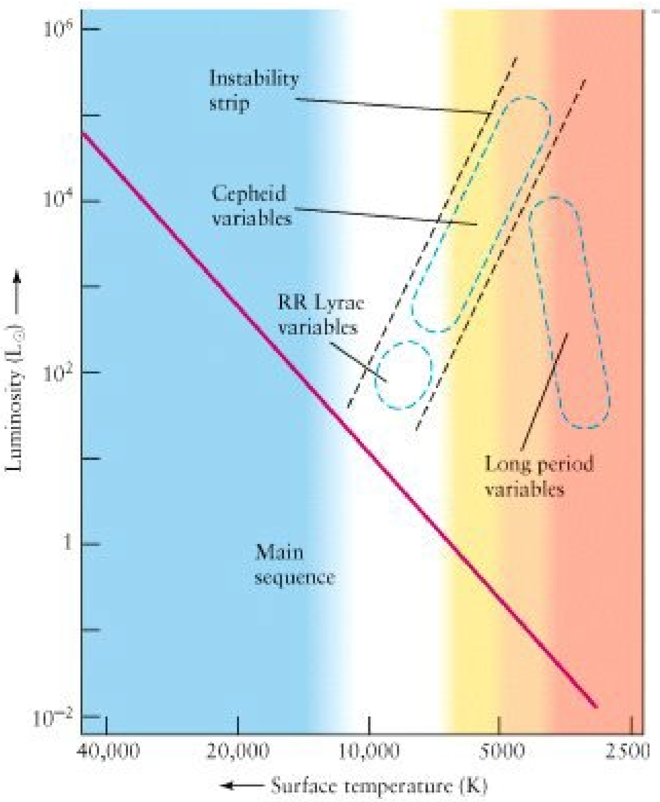

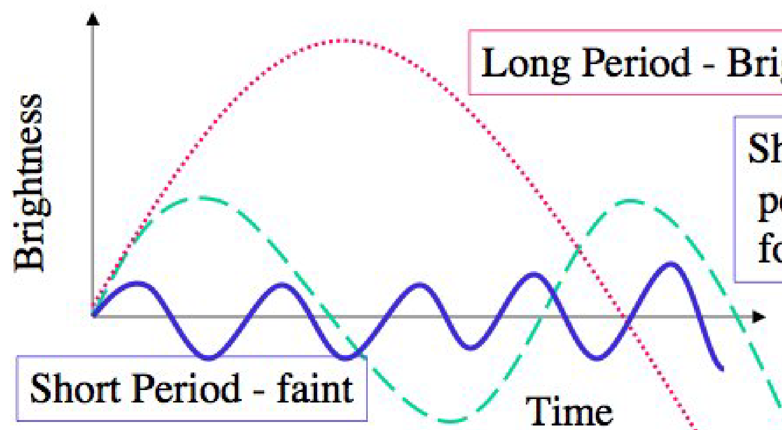

Shows relation of period and brightness for Cepheid variables.

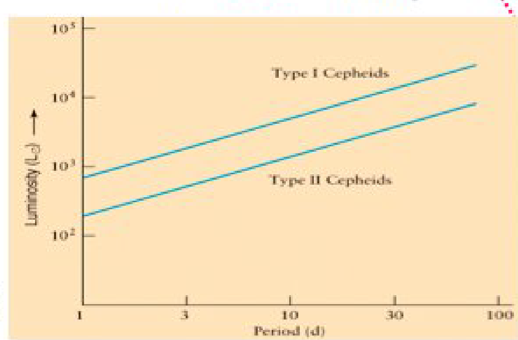

Note there are two Cepheid relations, with Type I in plane of Milky Way vs Type II in globular clusters.

October 5, 05

Primary distance indicators: Cepheids (<20 Mpc)

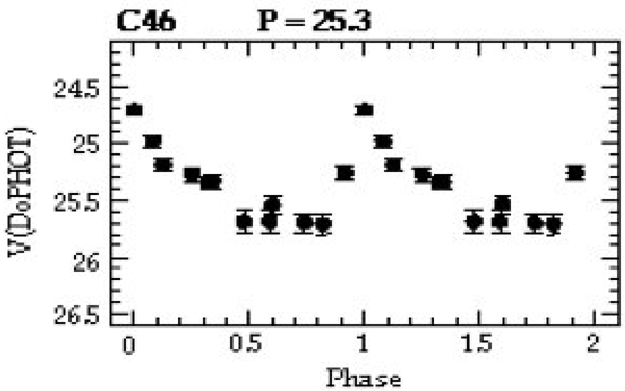

(Kelson et al. 1997)

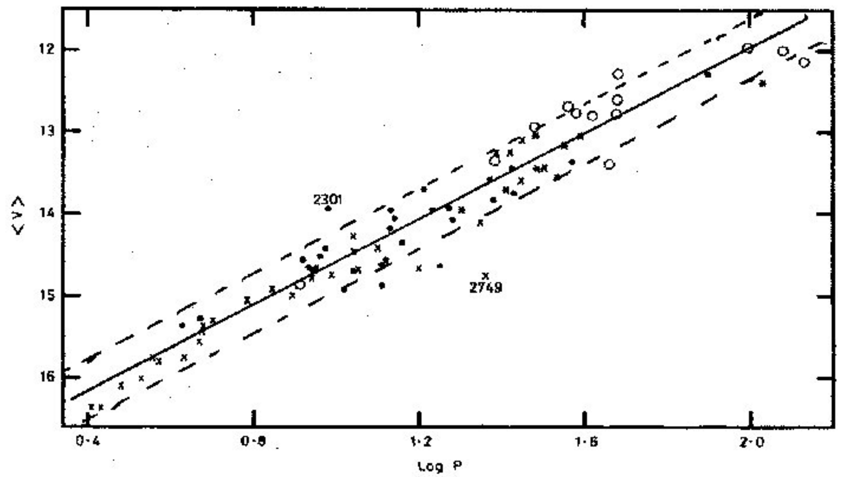

(Madore & Freedman 2001)

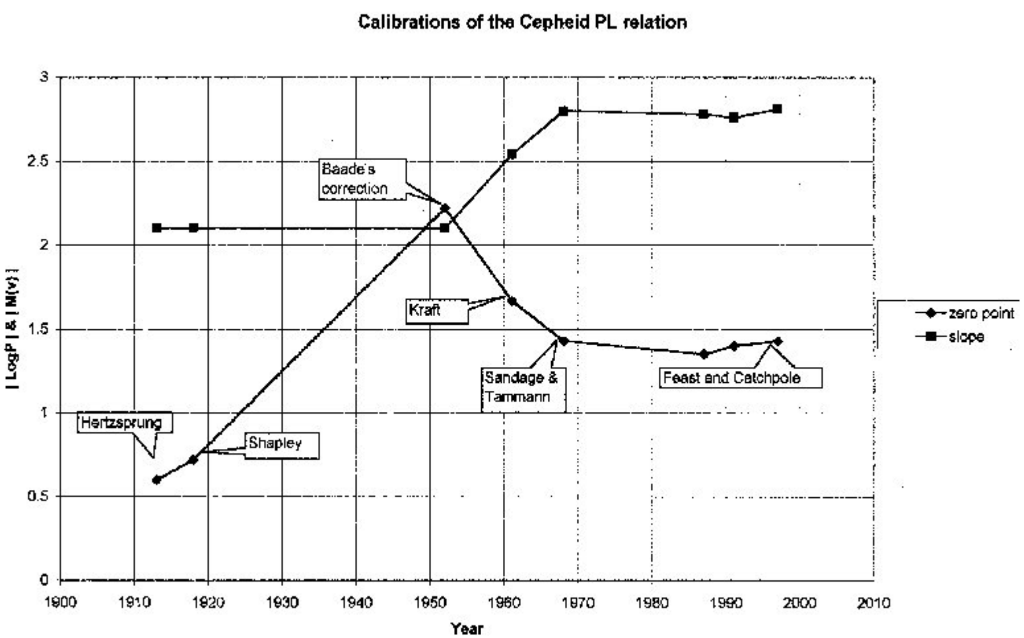

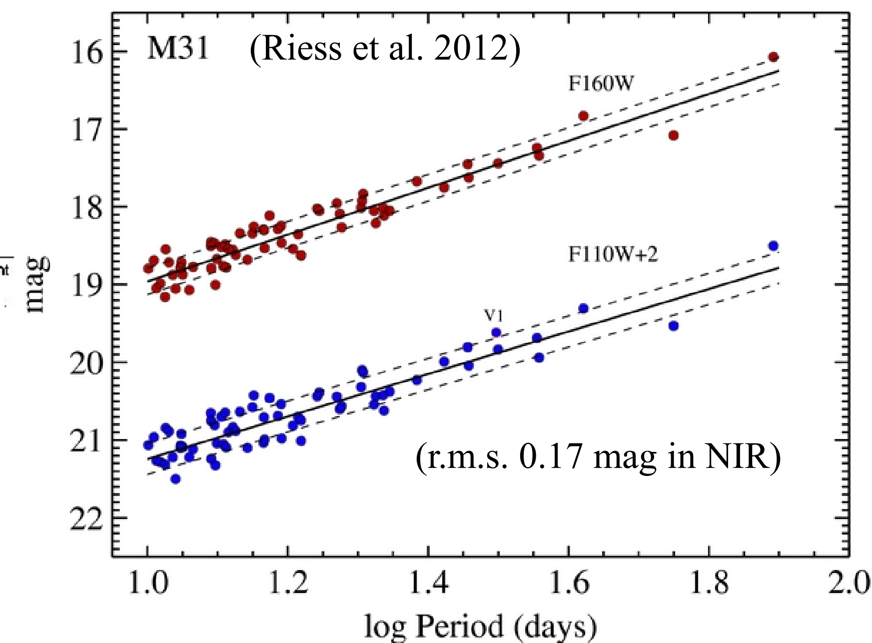

(Allen 2001: http://www.institute-of-brilliant-failures.com/index.htm)

Hubble-Lemaître Law

The furthest a galaxy, the largest the redshift $v=cz=H_0\,d$ (Lemaître 1927, Hubble 1929), where H_0 is Hubble´s constant that measures the rate at which the Universe expands (currently $H_0 \approx 70$ km/s/Mpc), and the definition of redshift $z \equiv (\lambda-\lambda_{em})/\lambda_{em}$

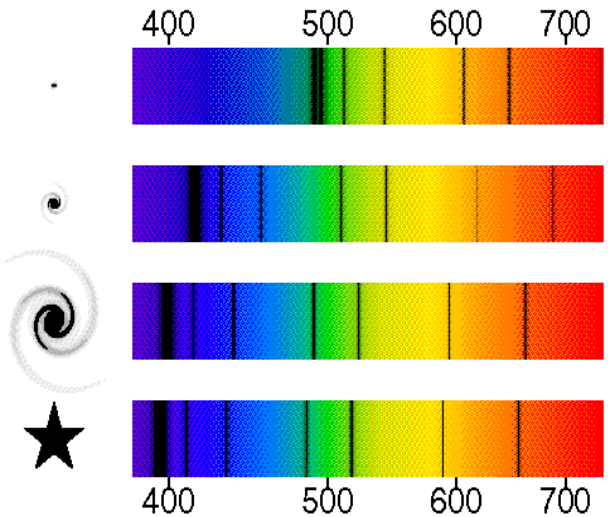

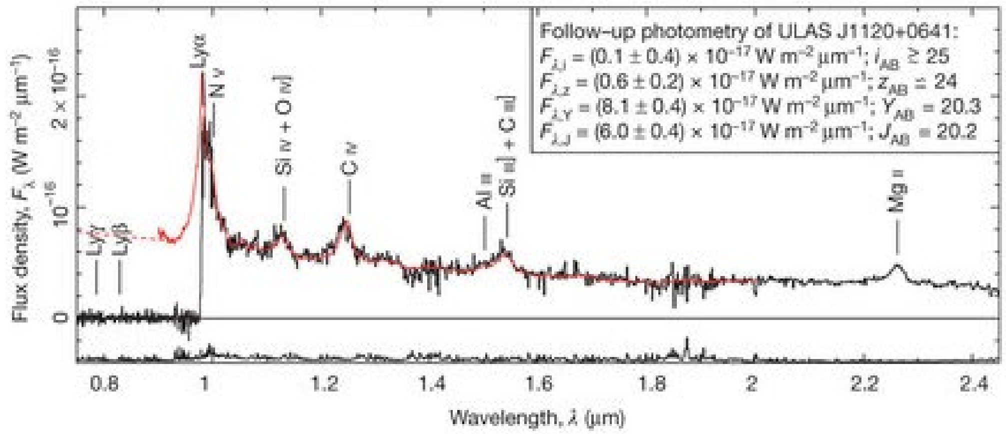

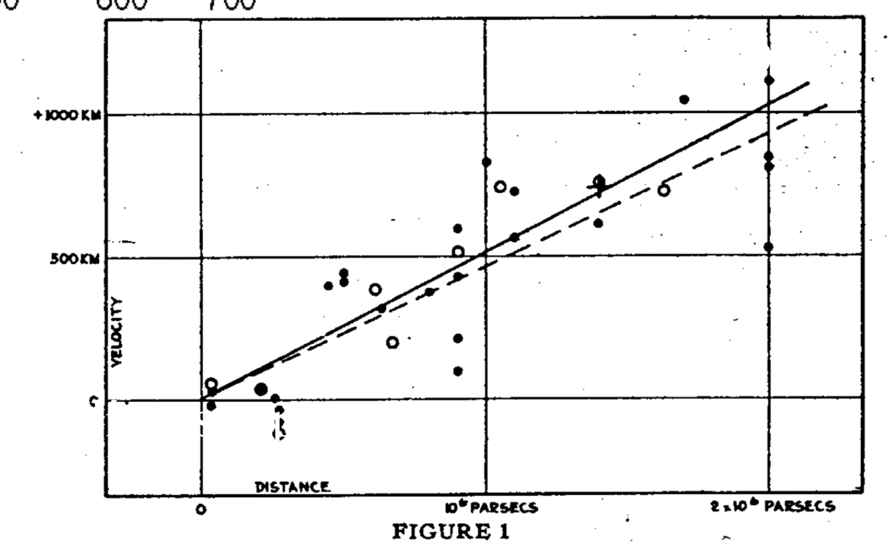

(Hubble 1929)

The birth of Cosmological Physics

- 1917 Albert Einstein: General Relativity

$$R_{\mu\nu} - \frac{1}{2} R \, g_{\mu\nu} + \Lambda \, g_{\mu\nu} = \frac{8 \pi G}{c^4} T_{\mu\nu}$$

- Developments by Willem de Sitter, Karl Schwarzchild, Arthur Eddington… and
- 1922 Alexander Friedman´s expanding universe solution
- 1927 George Lemaître´s “Primeval Atom”, independent of Friedman’s calculations
- 1930 Fred Hoyle in a BBC program coined the “Big Bang“ term

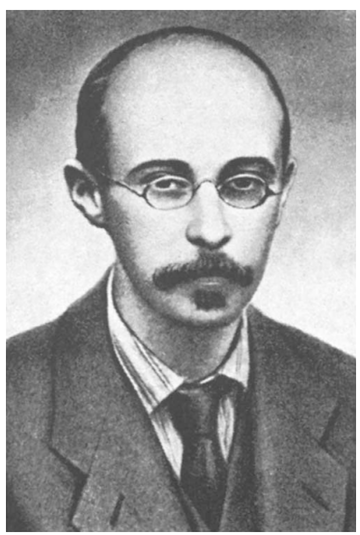

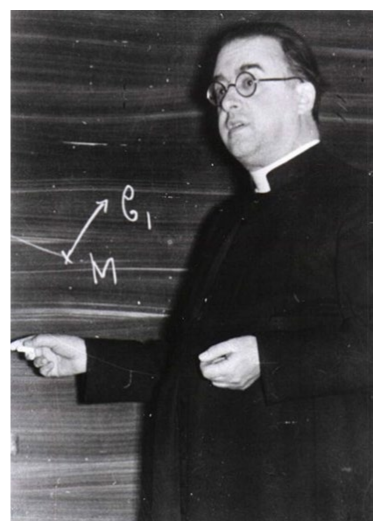

Basic cosmological equations to understand galaxies

Friedmann-Lemaître-Robertson-Walker (FLRW) metric (1922-1936), valid for an homogenous and isotropic Universe (Cosmological Principle)

$$ds^2 = c^2 dt^2 - R^2\left[\frac{dr^2}{1-kr^2} + r^2(d\theta^2 + \sin^2\theta d\phi^2)\right]$$

Definition of redshift $z \equiv (\lambda_o - \lambda_{em})/\lambda_{em}$

From the FLRW metric we derive $1+z = \frac{\lambda_0}{\lambda_{em}} = \frac{R_0}{R}$

And hence z is a direct measure of the ratio between the scale factors of the Universe now (R_0) and when the light we detect was emitted (R)

From Einstein´s Field Equations and the FLRW metric, we derive Friedman´s equations of motion $(\dot{R}, \ddot{R})$ and how to measure distances and time as a function of redshift (see http://www.astro.ucla.edu/~wright/CosmoCalc.html for a calculator):

$$d_m = R_0 r \approx \frac{1}{H_0}\int_0^z \frac{c\,dz}{\left[\Omega_M(1+z)^3 + \Omega_k(1+z)^2 + \Omega_\Lambda\right]^{1/2}}$$

proper distance today to a galaxy at redshift z

$$t_z = \frac{1}{H_0}\int_z^\infty \frac{dz}{(1+z)\left[\Omega_M(1+z)^3 + \Omega_k(1+z)^2 + \Omega_\Lambda\right]^{1/2}}$$

age of the Universe when the light departed from the galaxy

Extragalactic surveys: nearby Universe

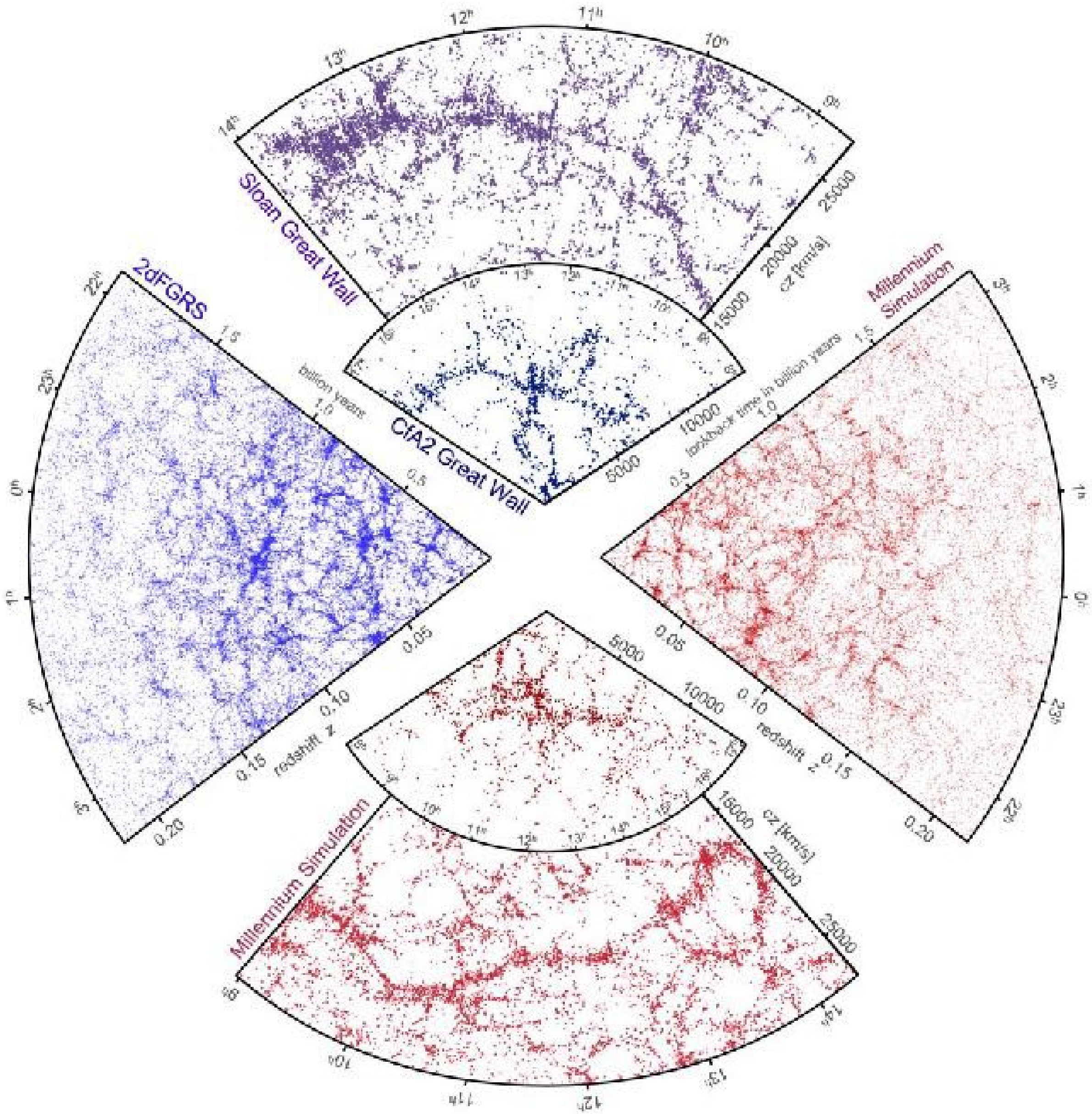

Galaxy Zoo

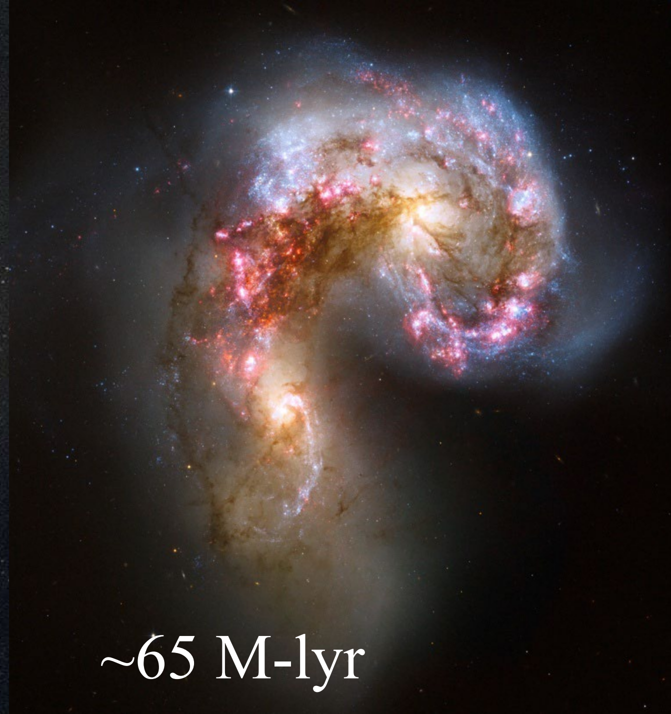

Elliptical galaxies (E)

Galaxies of this class have smoothly varying brightness, steadily decreasing outward from the center. They appear elliptical in shape. These galaxies are nearly all of the same color: they are somewhat redder than the Sun. Ellipticals are also almost devoid of cold gas or dust and contain mostly old stars.

cD galaxies, at the center of galaxy clusters are a special class of elliptical galaxy, much more massive and extended (R~1Mpc).

Spiral galaxies (S)

These galaxies are conspicuous for their spiral-shaped arms, which emanate from or near the nucleus and gradually wind outward to the edge. There are usually two opposing arms arranged symmetrically around the center. The nucleus of a spiral galaxy is a sharp-peaked area of apparent smooth texture, which can be quite small or, in some cases, can make up the bulk of the galaxy. The arms are embedded in a thin disk of stars. Both the arms and the disk of a spiral system are blue in color, whereas its central areas are red like an elliptical

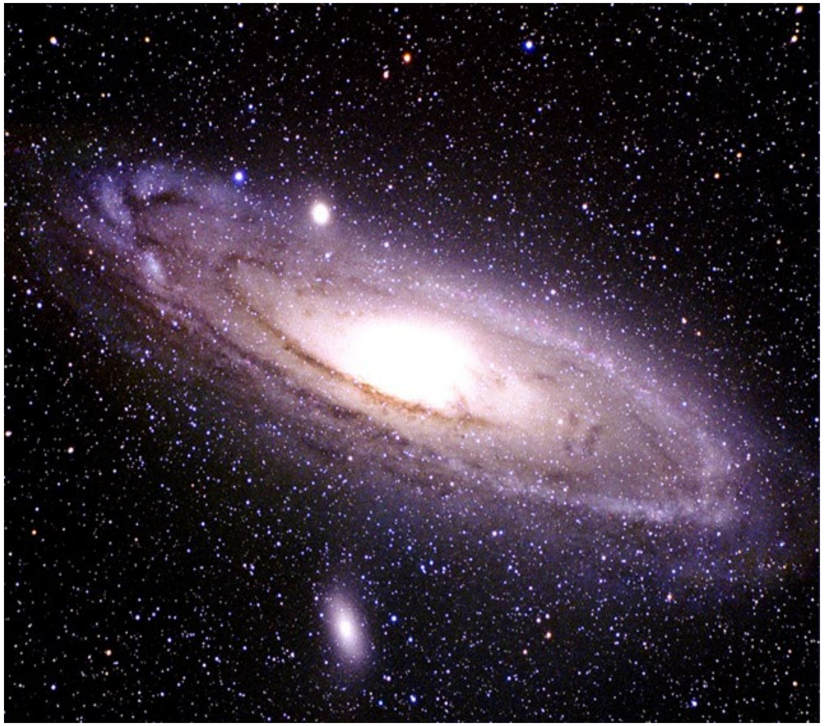

Irregular galaxies (Irr)

Most representatives of this class consist of grainy, highly irregular assemblages of luminous areas. They have no noticeable symmetry nor obvious central nucleus, and they are generally bluer in color than are the arms and disks of spiral galaxies.

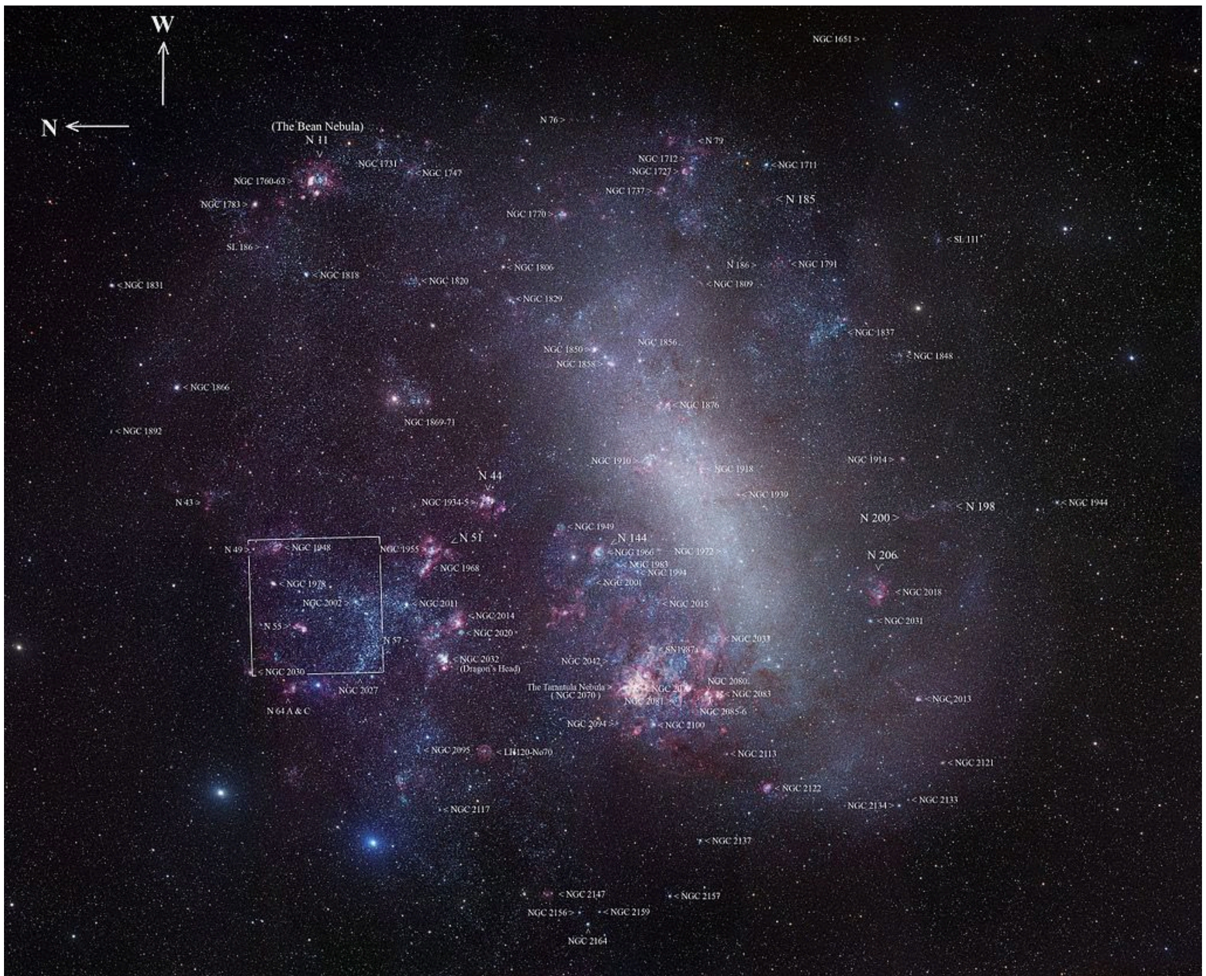

Emission mechanisms in galaxies

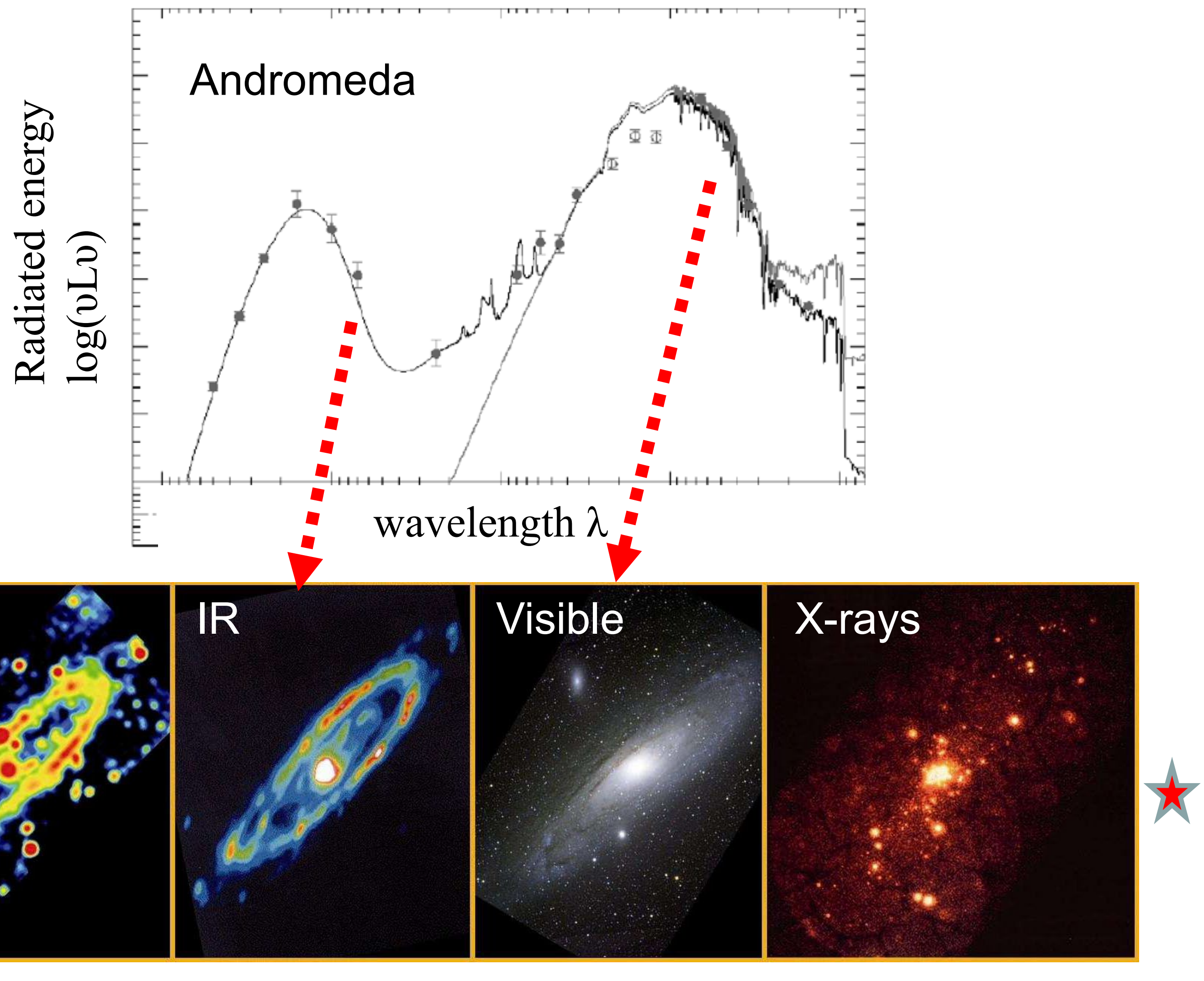

NON-THERMAL | THERMAL | NON-THERMAL
Sincrotron | Dust reemission, Stars | Sincrotron, inverse Compton
Bremsstralung | | Bremsstralung

Classification of galaxies

Hubble´s scheme refined by Sandage et al. (1975, see http://ned.ipac.caltech.edu/level5/Sandage/frames.html) based on appearence in photographs

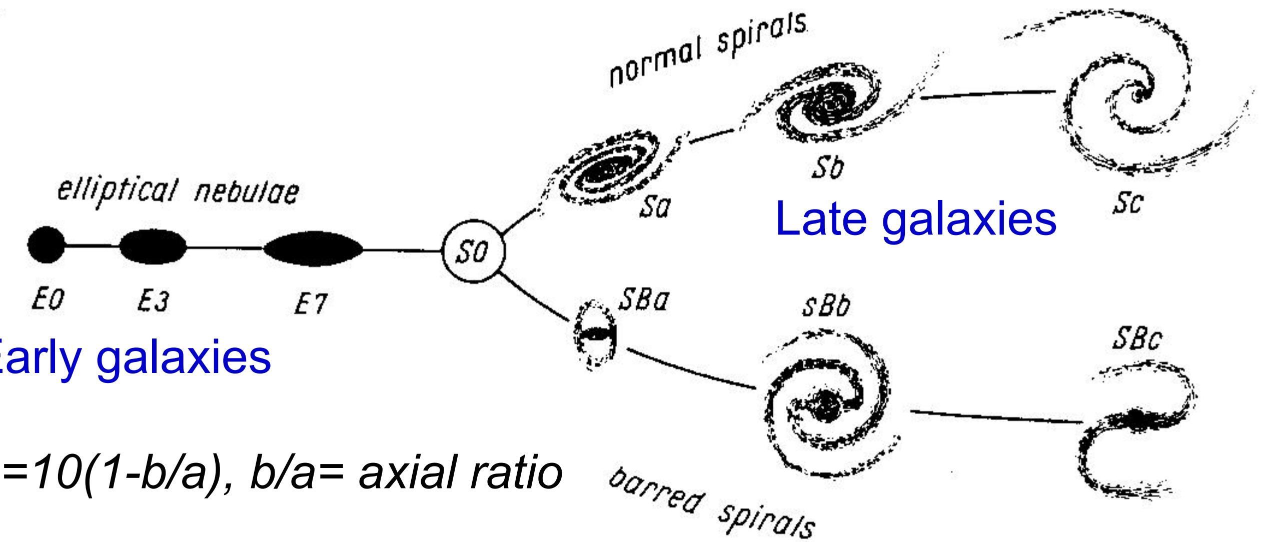

Early galaxies

Late galaxies

+ Irr

n=10(1-b/a), b/a= axial ratio

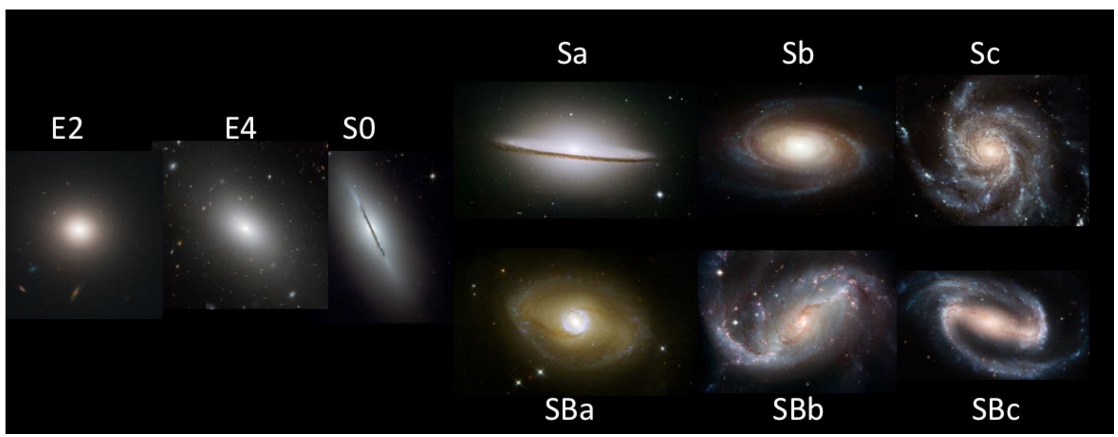

Decreasing bulge/disk ratio, gas content, star formation rate, ISM, less metal enriched

Classification of galaxies

Many other schemes are popular (see Bill Keel´s notes for a summary http://pages.astronomy.ua.edu/keel/galaxies/classify.html):

- De Vaucouleurs (1959) introduced continuity among spirals and irregulars, and description of the spiral structure as ringed (r) or purely spiral like (s).
  T=-4 (E), 1 (S0) 0 (S0/a), … 5 (Sc) … 9 (Im)
- Combes and Buta (1996) introduced a classification volumen based on the previous scheme

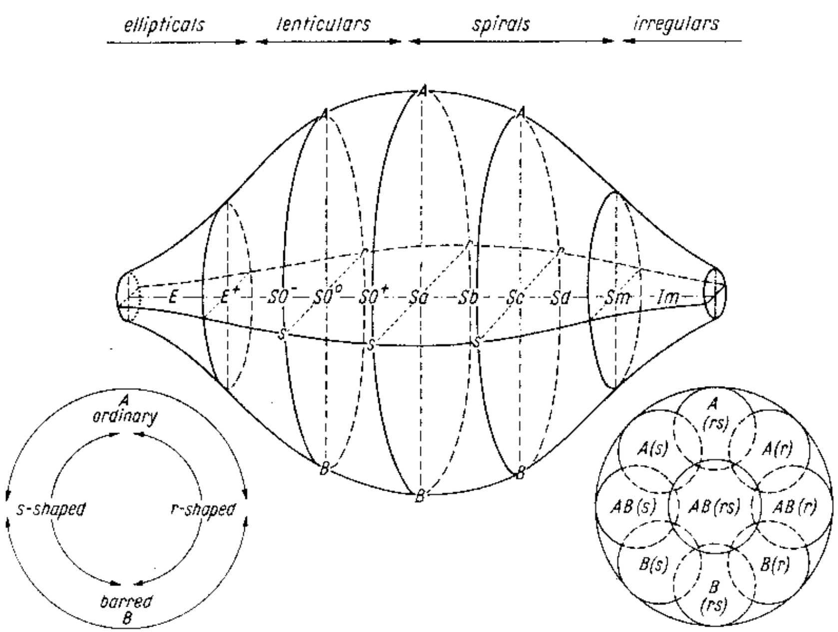

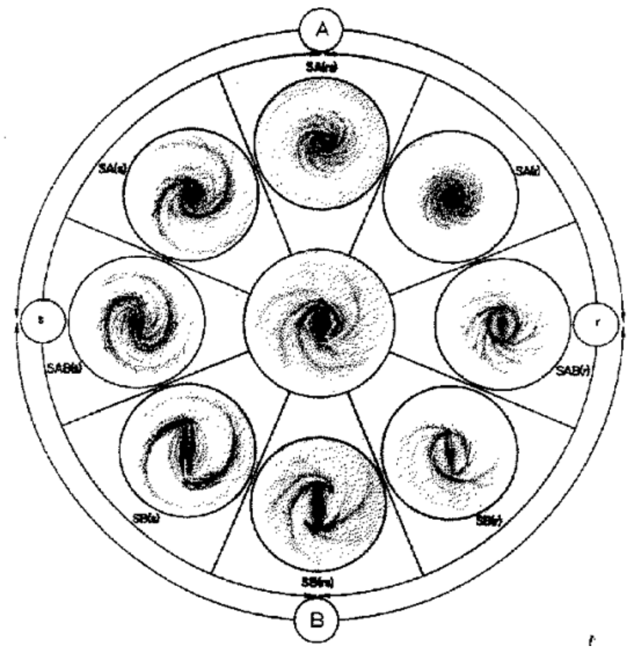

- Morgan: according to dominating stellar population
- Byurakan: according to concentration index, etc…

Classification of galaxies

T Hubble	-6	-5	-4	-3	-2	-1	0	1	2	3	4	5	6	7	8	9	10
de Vaucouleurs class	cE	E	E^+	$S0^-$	$S0^0$	$S0^+$	S0/a	Sa	Sab	Sb	Sbc	Sc	Scd	Sd	Sdm	Sm	Im
Hubble type aprox.	E			S0			S0/a	Sa	Sa-b	Sb	Sb-c	Sc			Sc-Irr	Irr I	

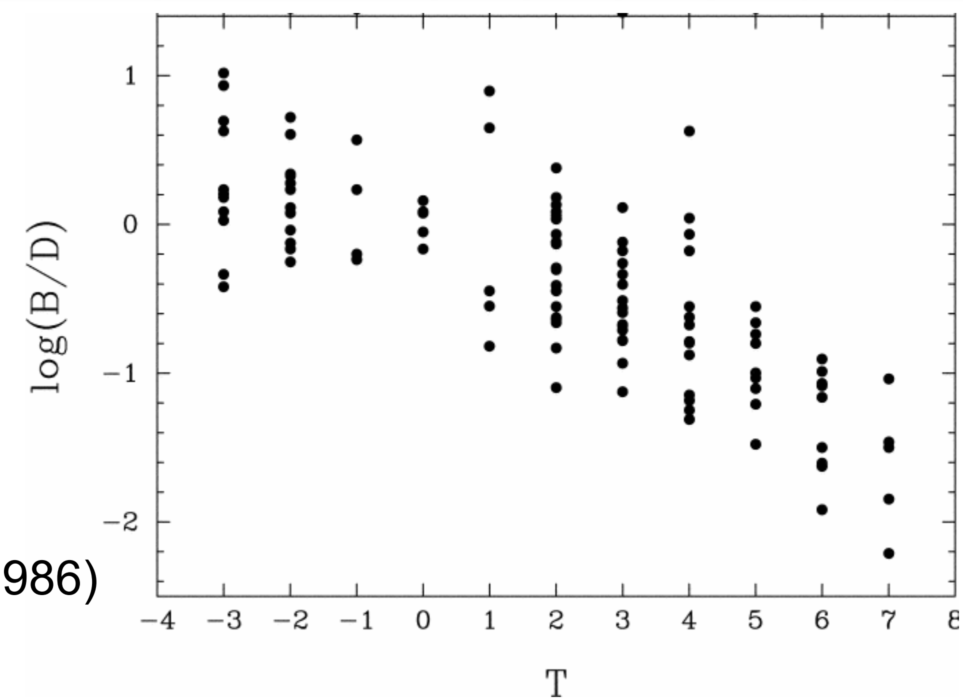

(Siemens & de Vaucouleurs 1986)

Morphological types in the nearby Universe

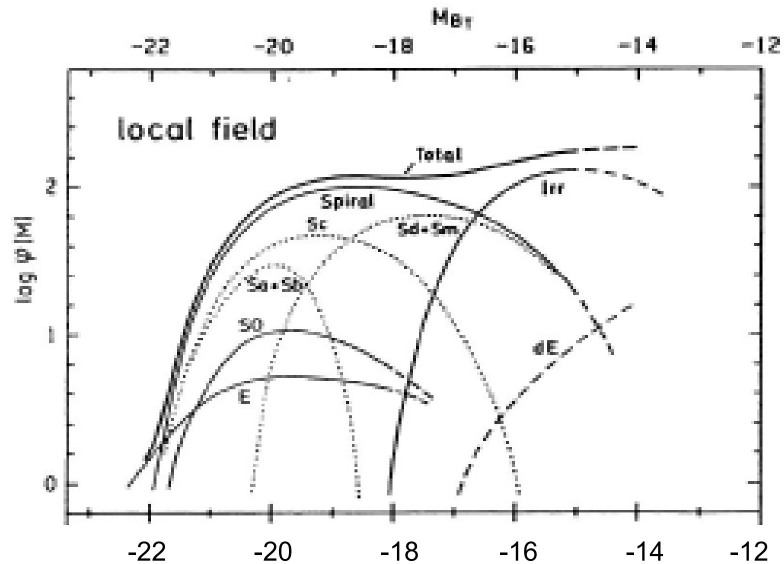

(Sandage 1990, in Clusters of Galaxies, CUP)

Morphology-Density Relation:

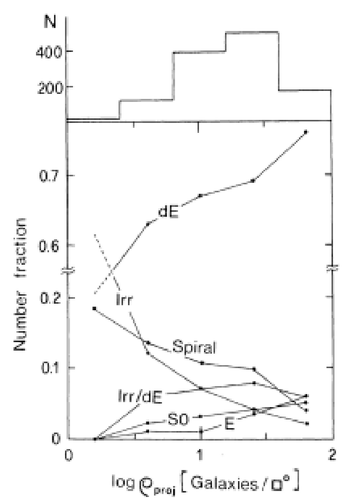

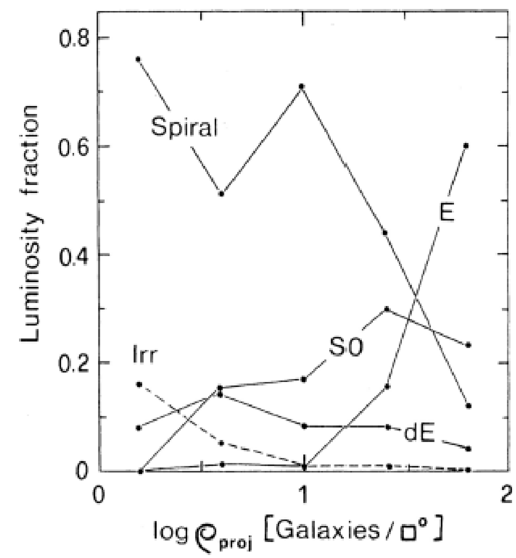

see: Binggeli et al. (1987) *AJ*, **94**, 251

Morphological types in the nearby Universe (z<0.2)

Sloan Digital Sky Survey (SDSS) DR7: 583362 galaxies at 55-565h^{-1} Mpc ($h \equiv H_0$/100 km/s/Mpc), S dominating population and strong environmental dependency in the field for E galaxies (Tempel et al. 2011)

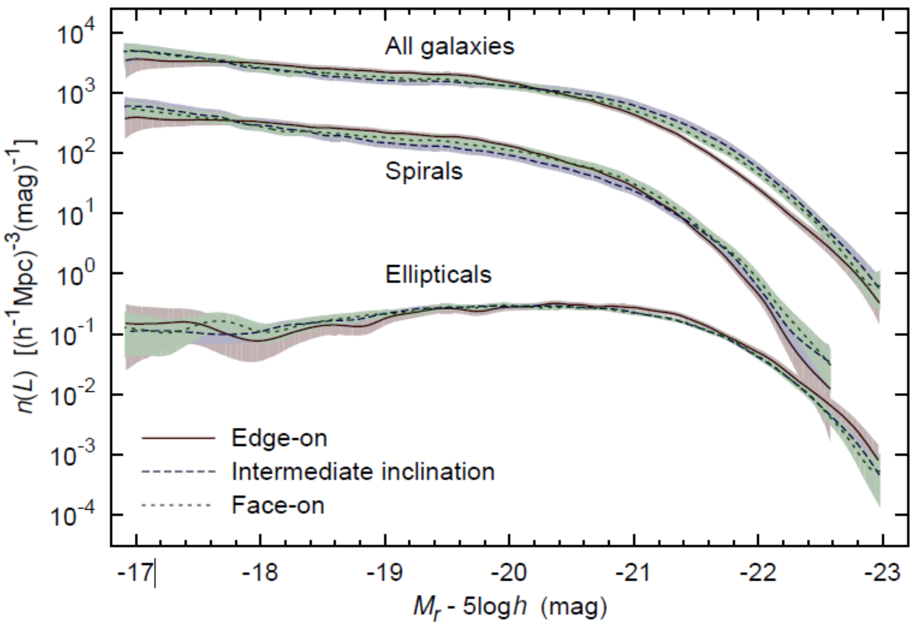

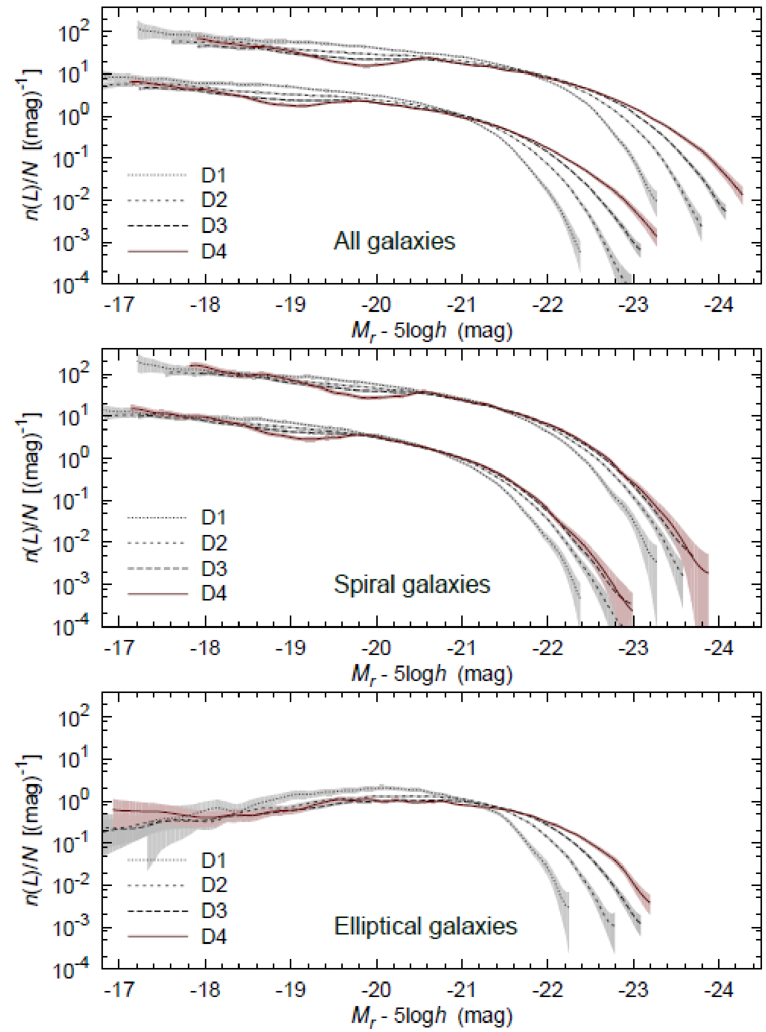

Notice that this luminosity function does not go as deep as the Nearby Universe one (which includes dwarf galaxies) because SDSS is a magnitude limited survey

Structural components

The structure of a galaxy can be derived from the analysis on its optical/IR surface photometry μ,*I* (mag arcsec^{-2} or mJy/beam, 1 Jy=10^{-26} W m^{-2} Hz^{-1}).

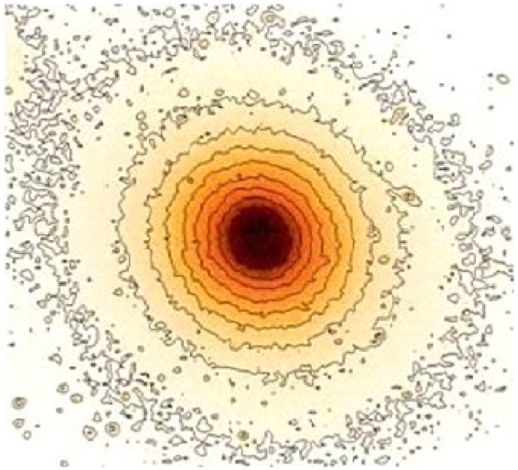

$$f = \frac{L}{4\pi d^2}$$ flux

$$\Omega = \frac{S}{d^2}$$ solid angle

We define $I = f/\Omega$ and $\mu=-2.5 \log I + c$ analogous to $m=-2.5 \log f + c$. I and μ are independent of distance for nearby galaxies (up to $z \approx 0.1$)

One can create isophotes joining areas with equal I, like top

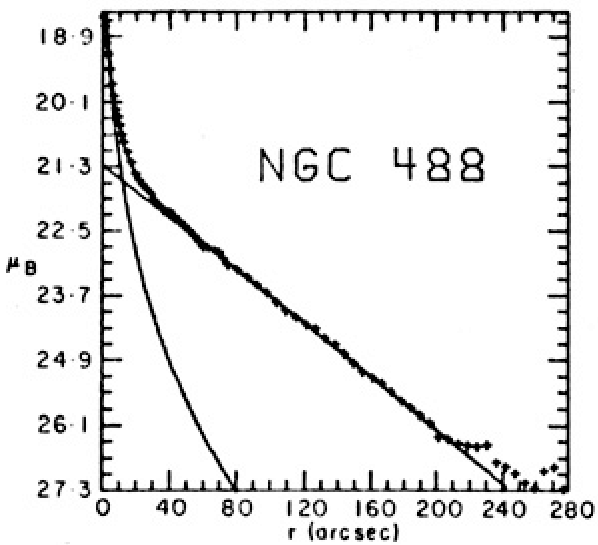

•*I(r)* actually comes from an azimuthal average, i.e of the light between isophotes of the same shape as the galaxy
• we do not always see the steep rise in the core – if a galaxy has a small core, the atmospheric seeing may blur it out to an apparent size equal to the seeing (e.g. 1 arcsec), And often central profiles are artificially flattened this way.

Structural components

Analyzing the isophotal information, several components emerge:

- **Bulge:** roughly spherical component, can be approximated by

$$I(r) = \frac{I_0}{(1 + r/a)^2}$$

Hubble-Reynold law (1930), empirical fit. Beware that L diverges if one integrates to large r, so it has to be truncated. I_0 is the central surface brightness and a is a reference radius.

$$I(r) = I_e \exp\left[-7.67\left(\frac{r}{r_e}\right)^{1/4} - 1\right]$$

de Vaucouleurs law (1958), also an empirical fit, where r_e is the radius that contains ½ light, and hence $L=22.4\, I_e\, r_e$.

$$\frac{I(r)}{I_0} = k\left[\frac{1}{(1 + (r/r_c)^2)^{1/2}} - \frac{1}{(1 + (r_t/r_c)^2)^{1/2}}\right]$$

King model (1978) for an auto-gravitating sphere with isotropic velocity dispersion, I_0 being the central surface brightness, r_c core radius, and r_t tidal radius

- **Disk:** thin flat structure, often expressed as an exponential law $I(r) = I_0 \exp(-r/r_0)$
- Both exponential and de Vaucouleurs profiles are special cases of Sérsic profiles (1968) $I(r) = I_e \exp\left(-b_n\left[(r/r_e)^{1/n} - 1\right]\right)$, where I_e and n are independent and b_n is given by

$$L(<r) = I_e r_e 2\pi n \frac{e^{b_n}}{(b_n)^{2n}} \gamma(2n, b_n (r/r_e)^{1/n})$$

Structural components

Comparison of profiles, Sérsic *n* often interpreted as

Elliptical: 1.5 < n < 20
Bulge: 1.5 < n < 10
Pseudo-bulge: 1 < n < 2
Bar: n~0.5
(bars <15% total L)
Disc: n~1

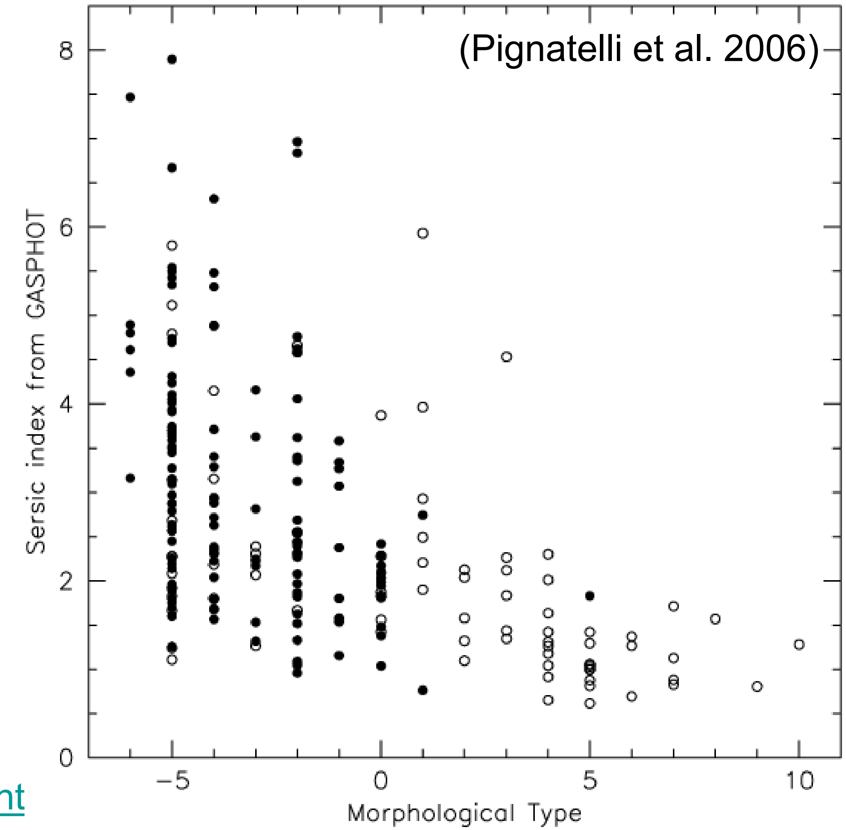

GALFIT (Peng et al. 2002, https://users.obs.carnegiescience.edu/peng/work/galfit/galfit.ht
an available code to fit surface brightness profiles in 2D

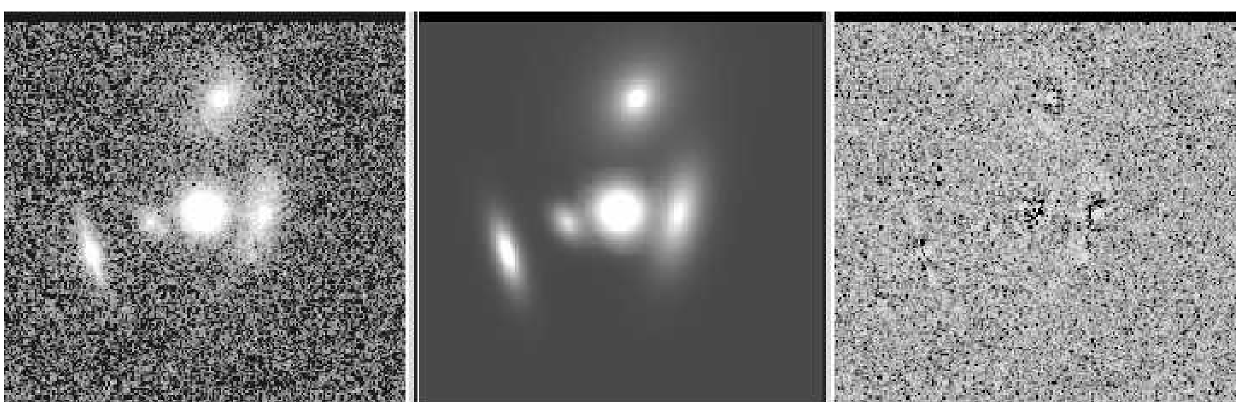

Structural components: non-parametric analysis

Light concentration of galaxies (Morgan 1962) 1st method. CAS (Conselice 2003, 2014 ARAA) is the most common method nowadays. It is based on the Petrosian (1976) radius : location where $I(r)/\langle I(<r)\rangle = \eta(r)$ such that $\eta(0)=1$, $\eta(\infty)=0$

I_0=original image, I_{180}=180deg rotated image, I_0^σ=smoothed (blurred) image by $\eta(r)=0.2$

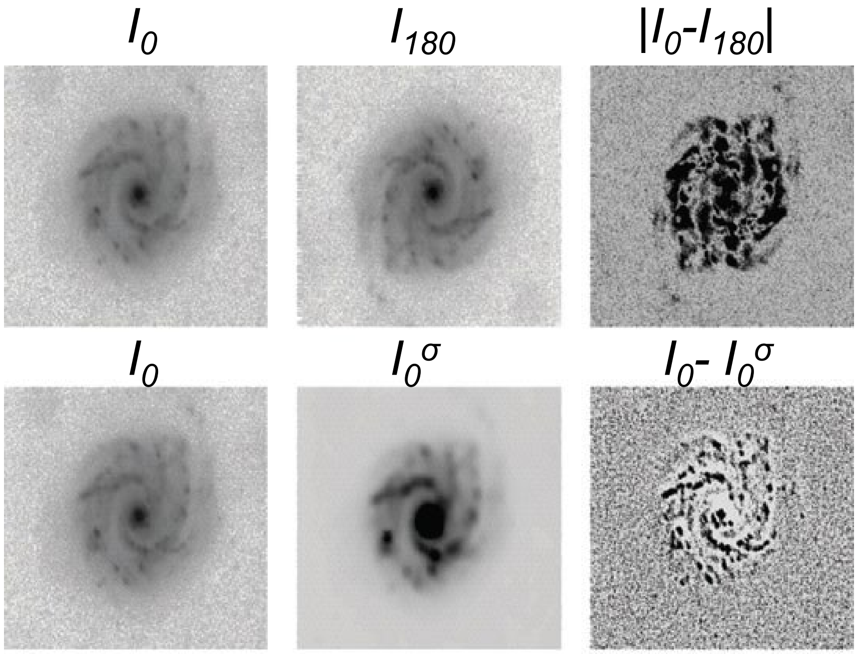

Asymmetry index:

$$A = min\left(\frac{\sum|I_0 - I_{180}|}{\sum|I_0|}\right) - min\left(\frac{\sum|B_0 - B_{180}|}{\sum|I_0|}\right)$$

Clumpiness index

$$S = 10 \times \left[\left(\frac{\sum(I_0 - I_0^\sigma)}{\sum I_0}\right) - \left(\frac{\sum(B_0 - B_0^\sigma)}{\sum I_0}\right)\right]$$

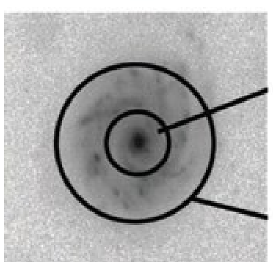

r_{20} for 20% of light

r_{80} for 80% of light

Concentration index

$$C = 5 \times \log_{10}\frac{r_{80}}{r_{20}}$$

Structural components: non-parametric analysis

For nearby galaxies (Conselice 2014 ARAA):

Galaxy type	Concentration	Asymmetry	Clumpiness
Ellipticals	4.4 ± 0.3	0.02 ± 0.02	0.00 ± 0.04
Early-type disks (Sa-Sb)	3.9 ± 0.5	0.07 ± 0.04	0.08 ± 0.08
Late-type disks (Sc-Sd)	3.1 ± 0.4	0.15 ± 0.06	0.29 ± 0.13
Irregulars	2.9 ± 0.3	0.17 ± 0.10	0.40 ± 0.20
Edge-on disks	3.7 ± 0.6	0.17 ± 0.11	0.45 ± 0.20
Dwarf ellipticals	2.5 ± 0.3	0.02 ± 0.03	0.00 ± 0.06

$$A = min\left(\frac{\sum|I_0 - I_{180}|}{\sum|I_0|}\right) - min\left(\frac{\sum|B_0 - B_{180}|}{\sum|I_0|}\right)$$

$$C = 5 \times \log_{10}\frac{r_{80}}{r_{20}}$$

$$S = 10 \times \left[\left(\frac{\sum(I_0 - I_0^{\sigma})}{\sum I_0}\right) - \left(\frac{\sum(B_0 - B_0^{\sigma})}{\sum I_0}\right)\right]$$

Structural components: sizes

μ is the surface Brightness i.e. brightness per unit area

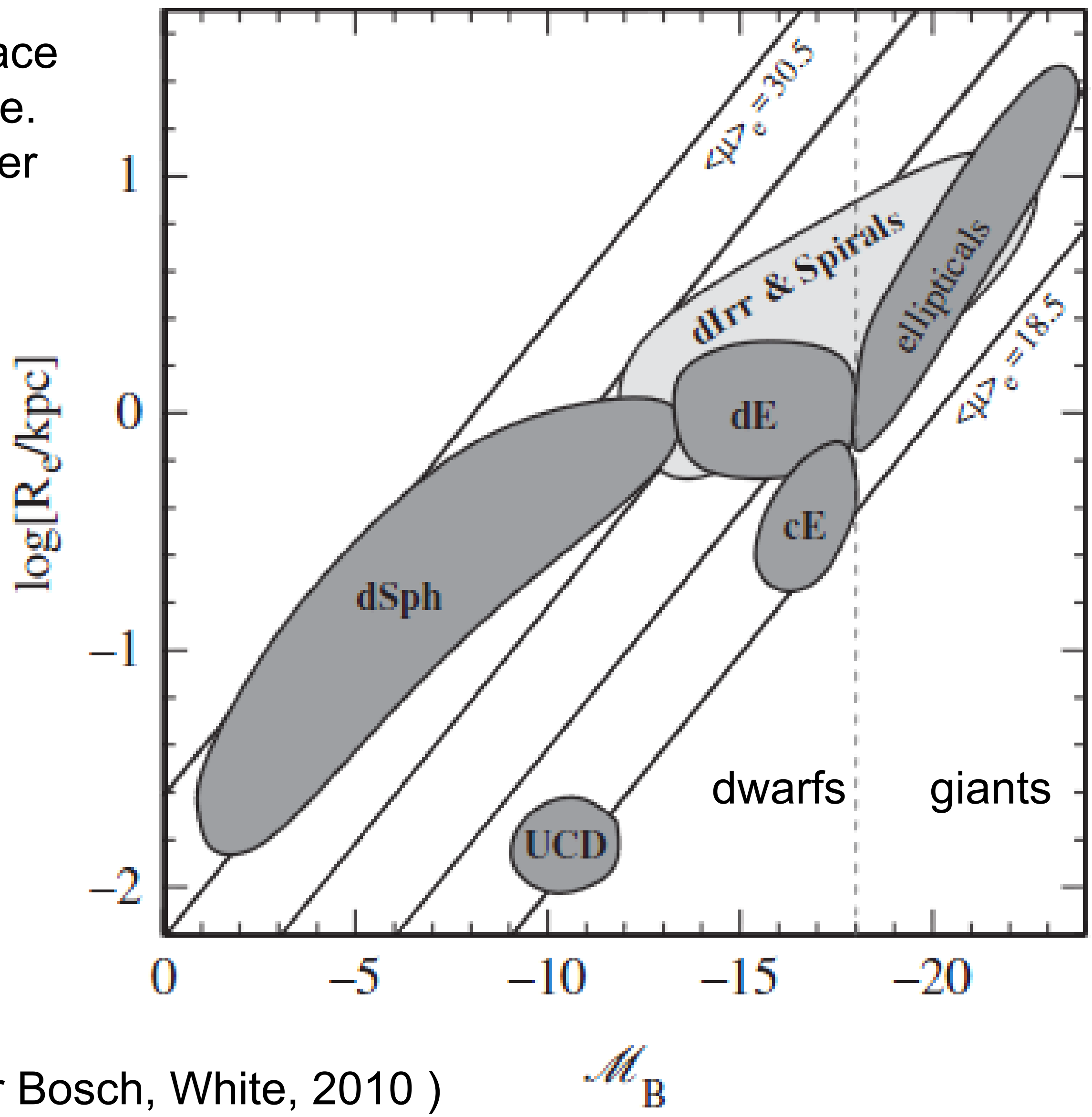

(Mo, van der Bosch, White, 2010)

Structural components: stellar kinematics

$$(V/\sigma)^* \equiv \frac{(v_{rot}/\sigma)}{(v_{rot}/\sigma)_{iso}} = \frac{(v_{rot}/\sigma)}{\sqrt{\frac{1-\varepsilon}{\varepsilon}}}$$

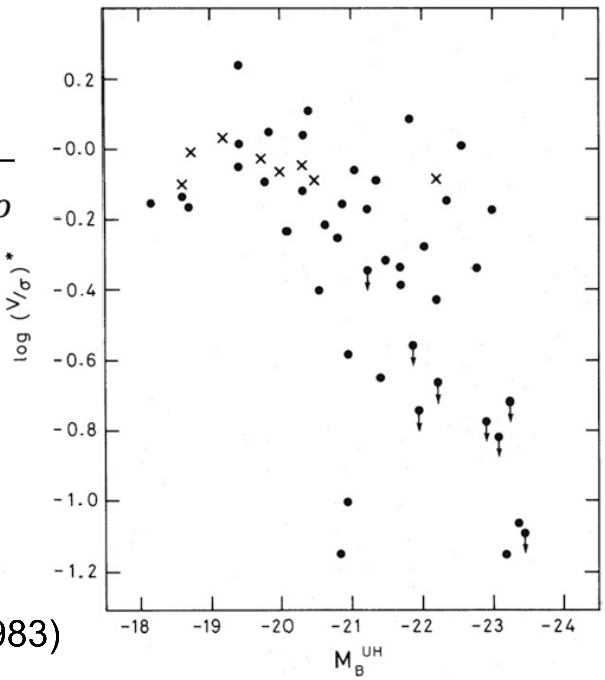

(Davis et al, 1983)

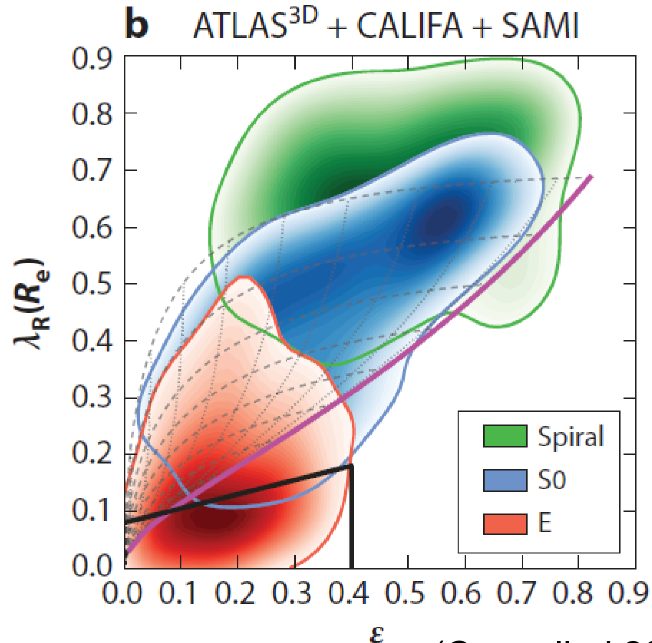

(Cappellari 2016, ARAA)

$$\lambda_R \equiv \frac{\langle |V| R \rangle}{\langle R\sqrt{V^2+\sigma^2}\rangle} = \frac{\sum F_i R_i |V_i|}{\sum F_i R_i \sqrt{V_i^2+\sigma_i^2}}$$

The disks of spiral galaxies are suported against collapse by rotation. We can measure their rotation curves by using the line-of-sight Doppler-shifts of emission and absorption lines.

Ellipticals have two components: a net rotation about their minor axis, and a strong component of random motion. Most ellipticals have triaxial shapes and are supported by anisotropic velocity dispersion.

Some spiral galaxies have pseudobulges, which follow exponential profile, are typically flatter, and have significant rotational support.

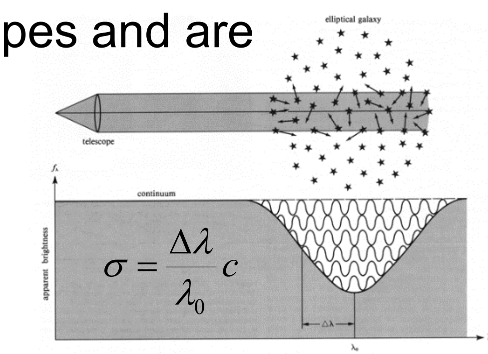

Stellar atmospheres

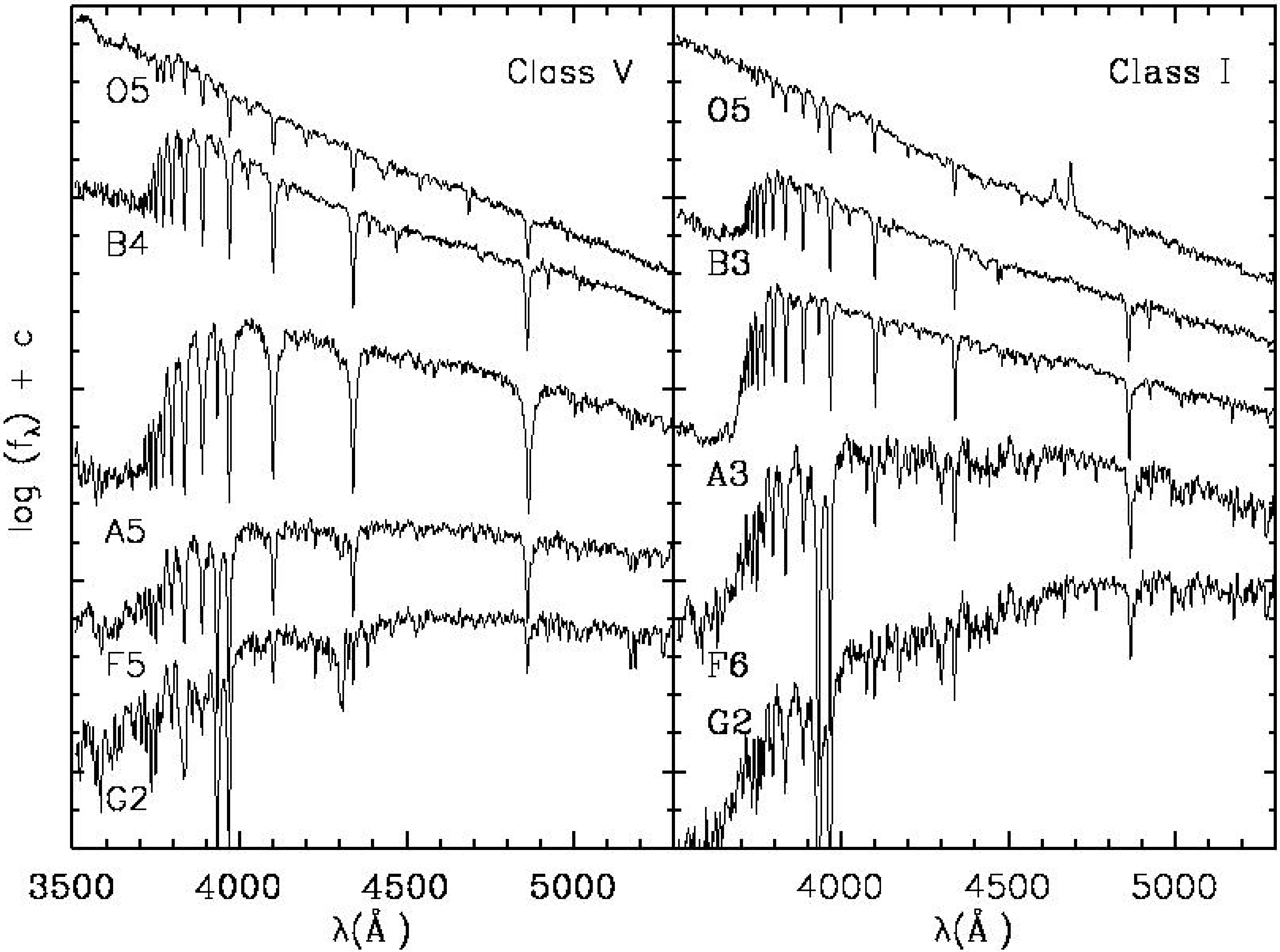

(from Jacoby et al. 1984)

Stars in galaxies

Based on their optical spectra:

- Elliptical galaxies are characterized by strong absorption lines, due to metals in the stellar atmospheres of the low luminosity stellar population. We see few to no emission lines ([OII]3727A and/or [NII]6583A are occasionally present), as there are very few young stars and little cold gas.

- Spiral galaxies are characterized by strong emission lines, due to young stars which heat and ionize the surrounding gas, and by absorption features due to the older, underlying stellar population.

- Blue (Magellanic type) irregular galaxies are characterized by strong emission lines, due to hot young stars and surrounding HII regions.

(Spectra from Kenicutt´s atlas 1992, ApJ, 388, 310, description from Nicole@UNM)

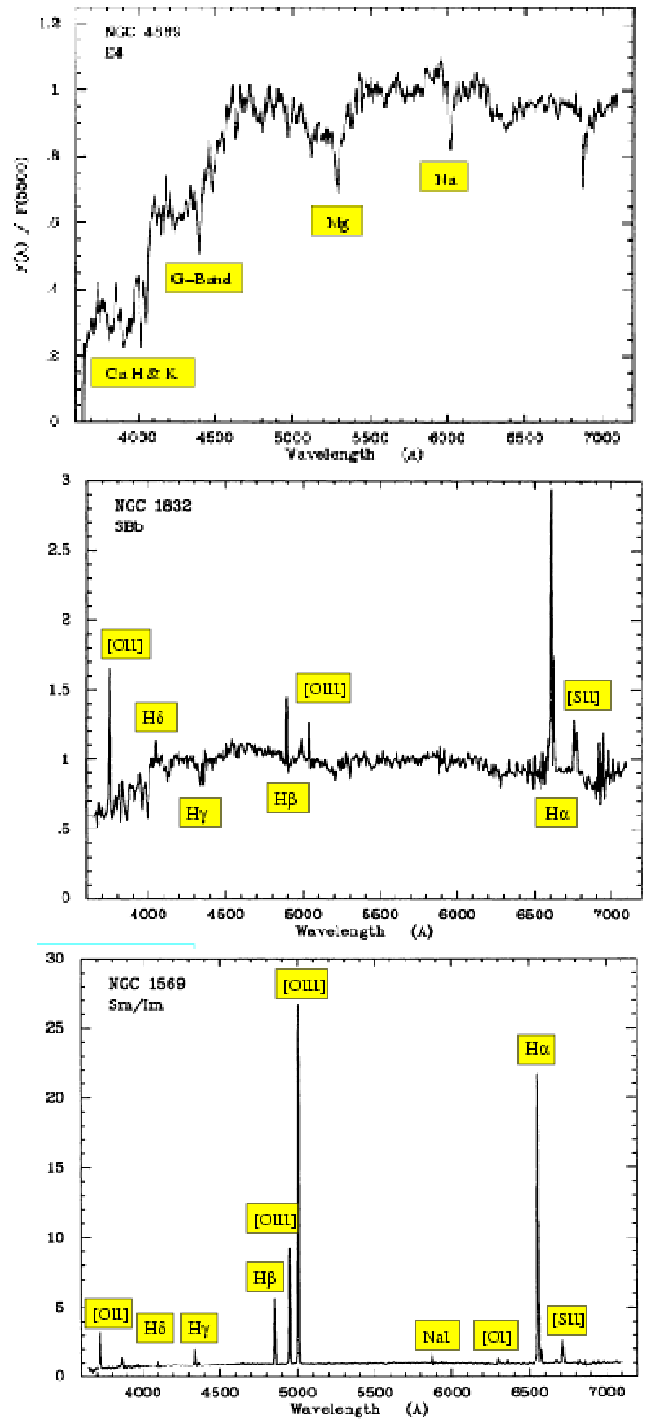

Stars in galaxies: spectral synthesis

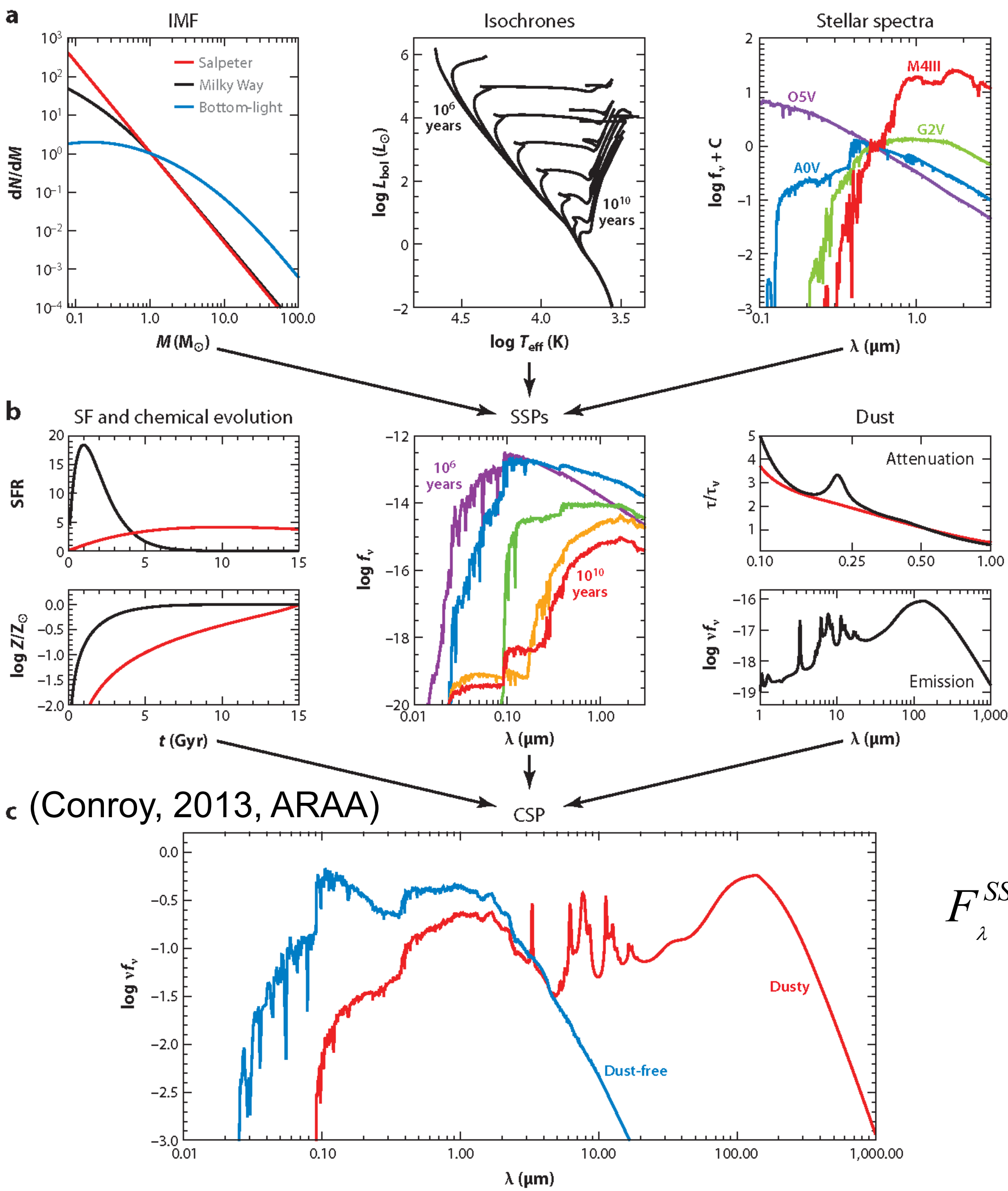

(Conroy, 2013, ARAA)

The Initial Mass Function (IMF), describes the abundance of stars per unit mass $dN/dm = \phi(m) = m^{-\alpha}$ such that the total stellar mass is

$$M = a \int_{m_l}^{m_u} m\phi(m)dm$$

A Single Stellar Population (SSP) is the most simple synthesized spectrum for a galaxy: given an age and the evolutionary stage of all stars (isochrone) in the H-R diagram (T_{eff} vs L), integrate the spectrum of all stars weighted by their relative numbers per mass

$$F_\lambda^{SSP}(t) = a \int_{m_l}^{m_u(t)} f_\lambda^*(T_{eff}(m), L(m,t))\phi(m)dm$$

Composite Stellar Populations (CSP) use a star formation (SF) funcion dependent on time

Popular Simple Stellar Population models

Wide selection of SSP models available for a general user, e.g.:

- Bruzual & Charlot (2003), good for old and intermediate populations
- Maraston (2005)
- PEGASE (Fioc & Rocca-Volmerange 1997)
- STARBURST99 (Leitherer et al. 1999), good for Young t<100 Myr populations
- FSPS (Flexible Stellar Population Synthesis) (Conroy, Gunn & White 2009)

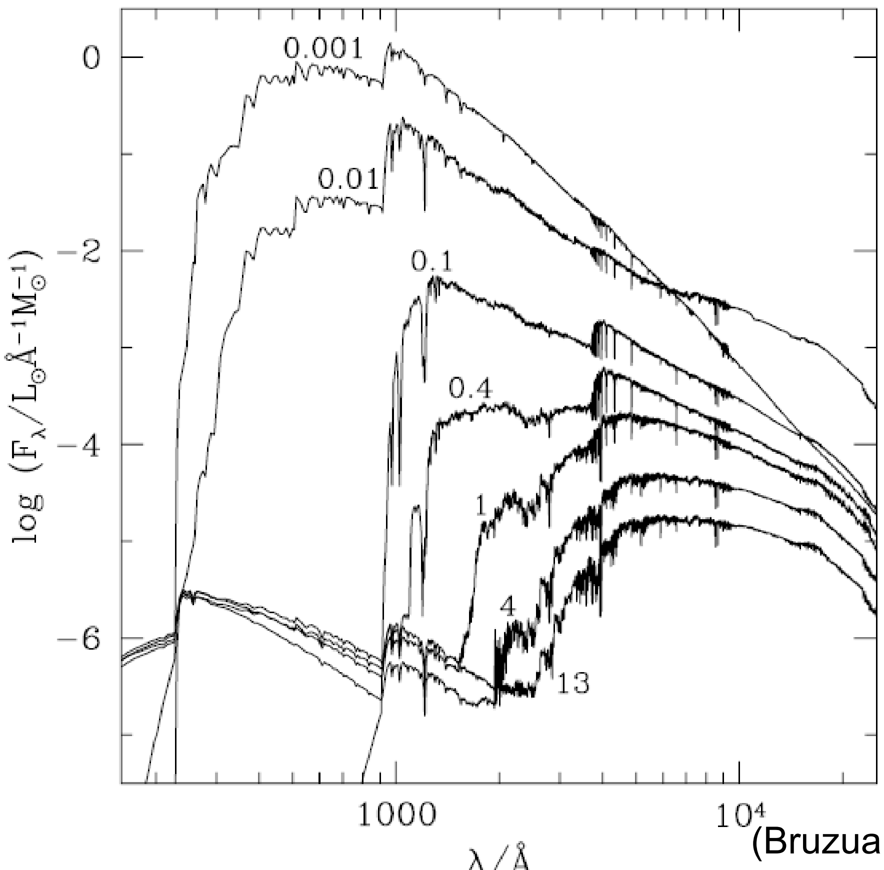

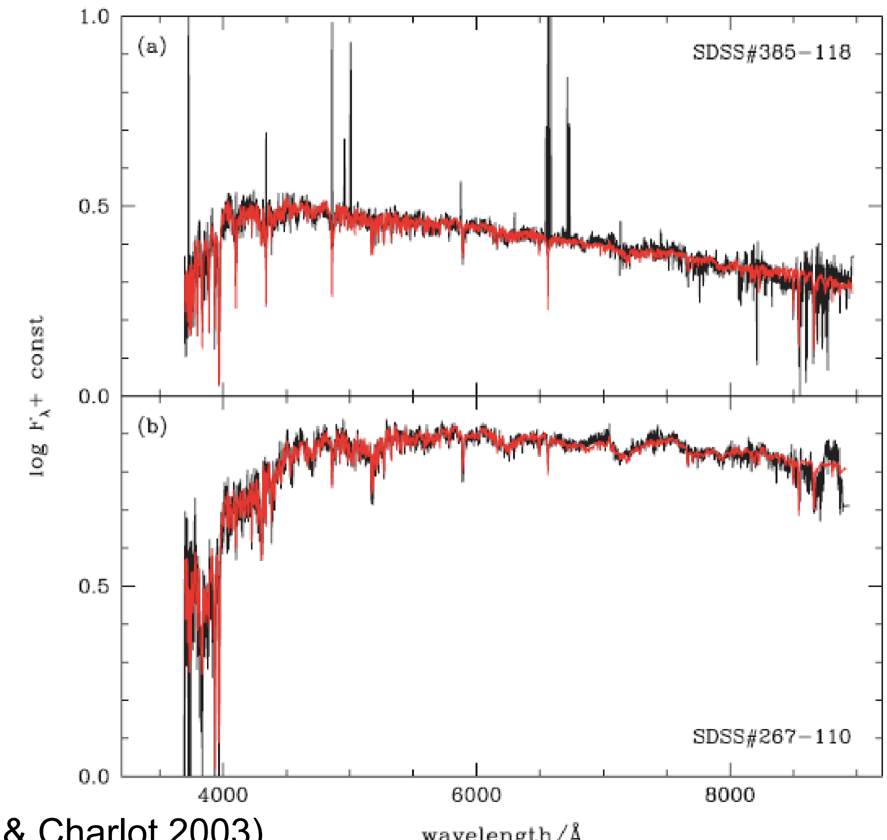

(Bruzual & Charlot 2003)

Stellar Population analysis: Lick Indices

Selected absorption lines in galaxies (Mg2, Fe5270, Hβ…) can be associated with fundamental parameters, like age or metallicity of a SSP

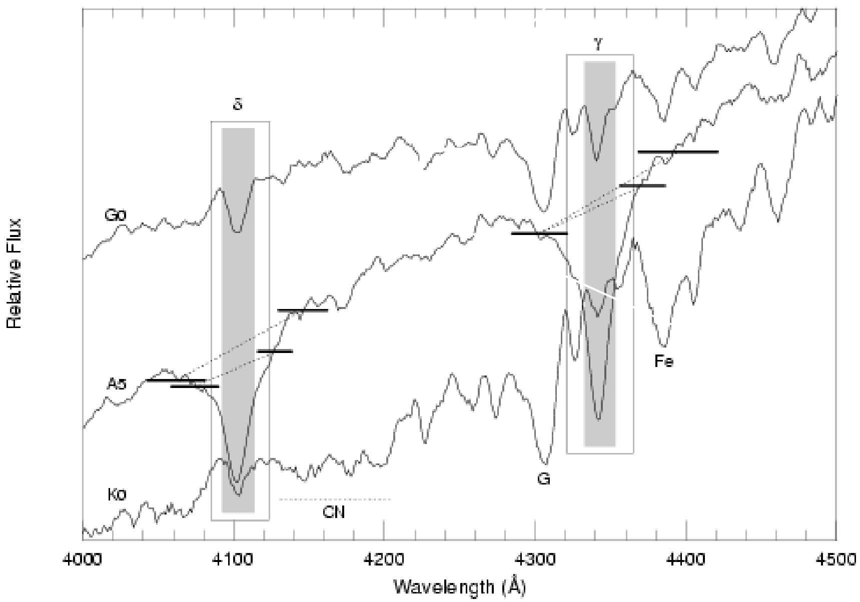

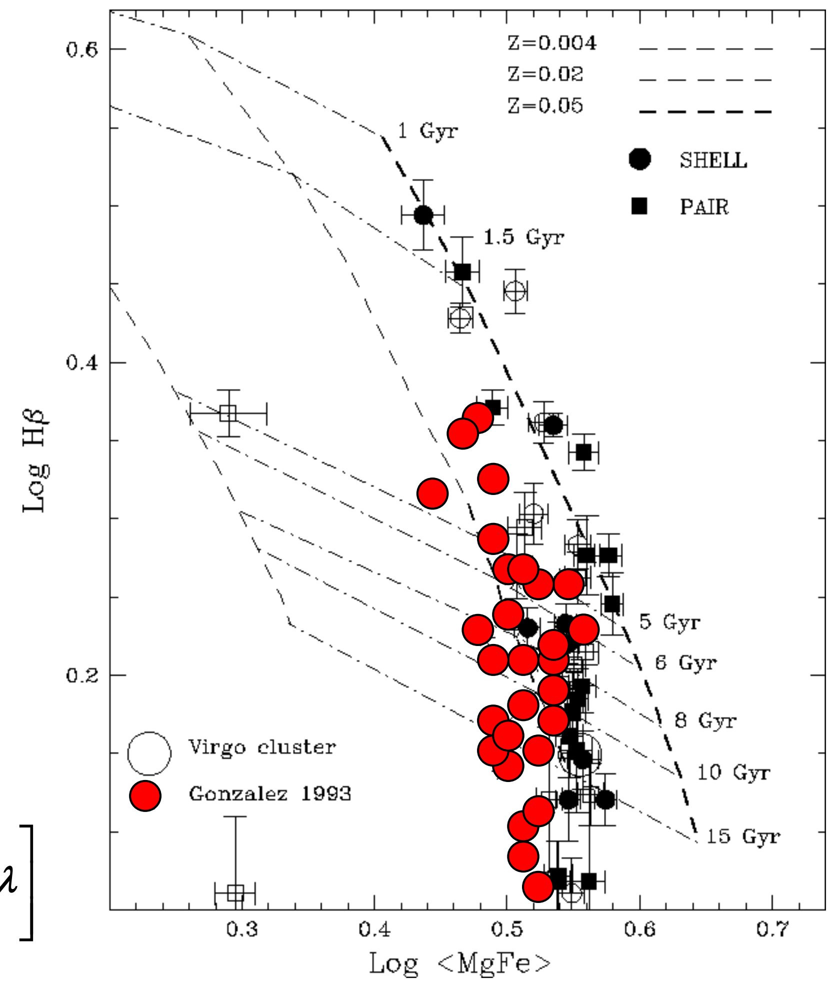

(Longhetti+1999)

Definition of indices (Worthey et al. 1994):

As Equivalent Widths (EW) $$EW = \int_{\lambda_1}^{\lambda_2} \left(1 - \frac{F_l}{F_c}\right) d\lambda$$

Or Magnitudes $$Mag = -2.5 Log\left[\frac{1}{\Delta\lambda}\int_{\lambda_1}^{\lambda_2} \frac{F_l}{F_c} d\lambda\right]$$

Stellar masses of galaxies

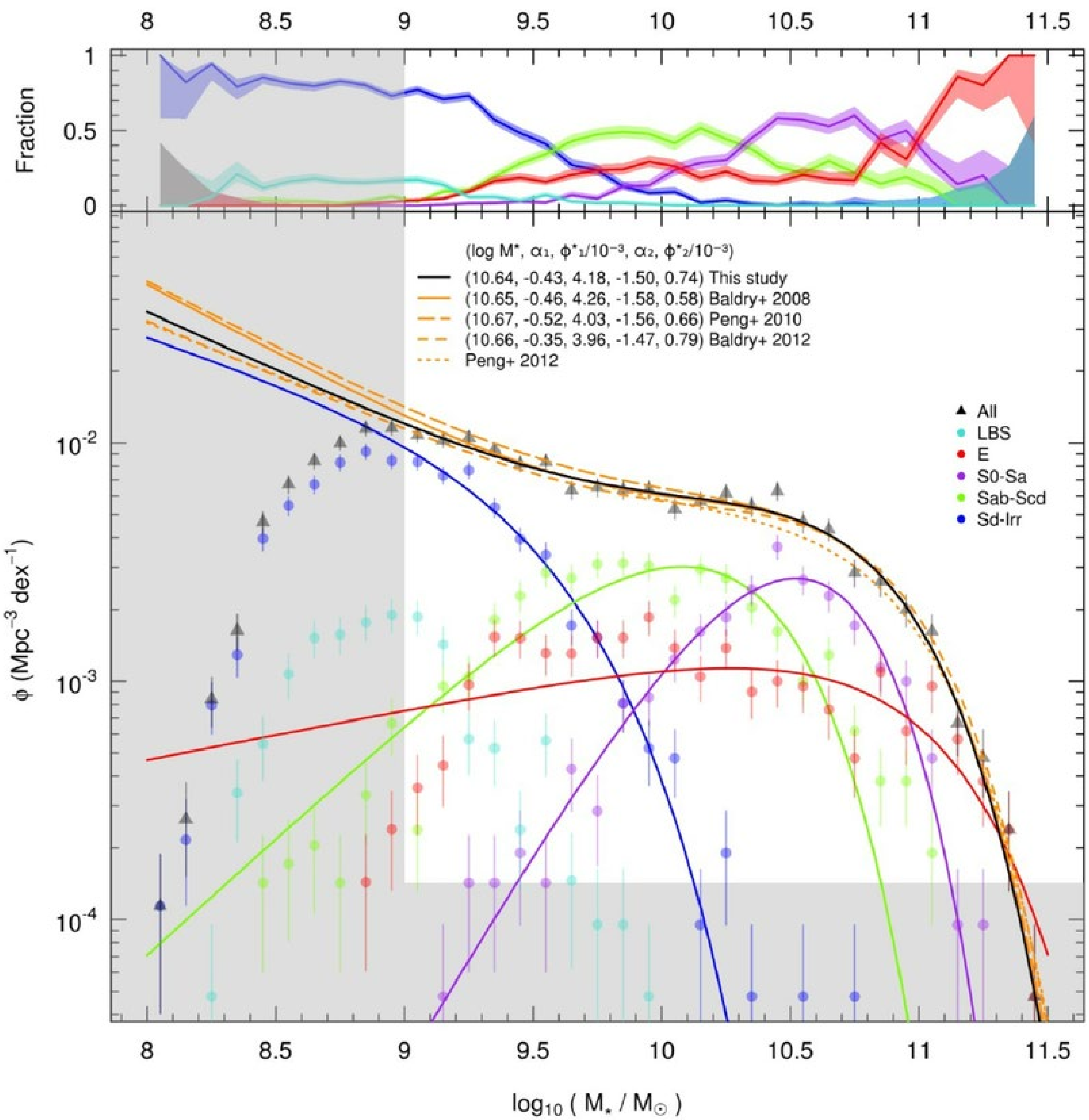

SSP gives us the stellar mass in galaxies (and a fair approximation can be derived from a scaling of the flux at IR bands (~K), where all stars contribute)

Mass functions of galaxies in a stellar mass limited sample

At logM>9 of ~3700 galaxies in the at 0.025<z<0.06 over ~286 deg2

(Kevin et al. 2014):

Radial ages of galaxies

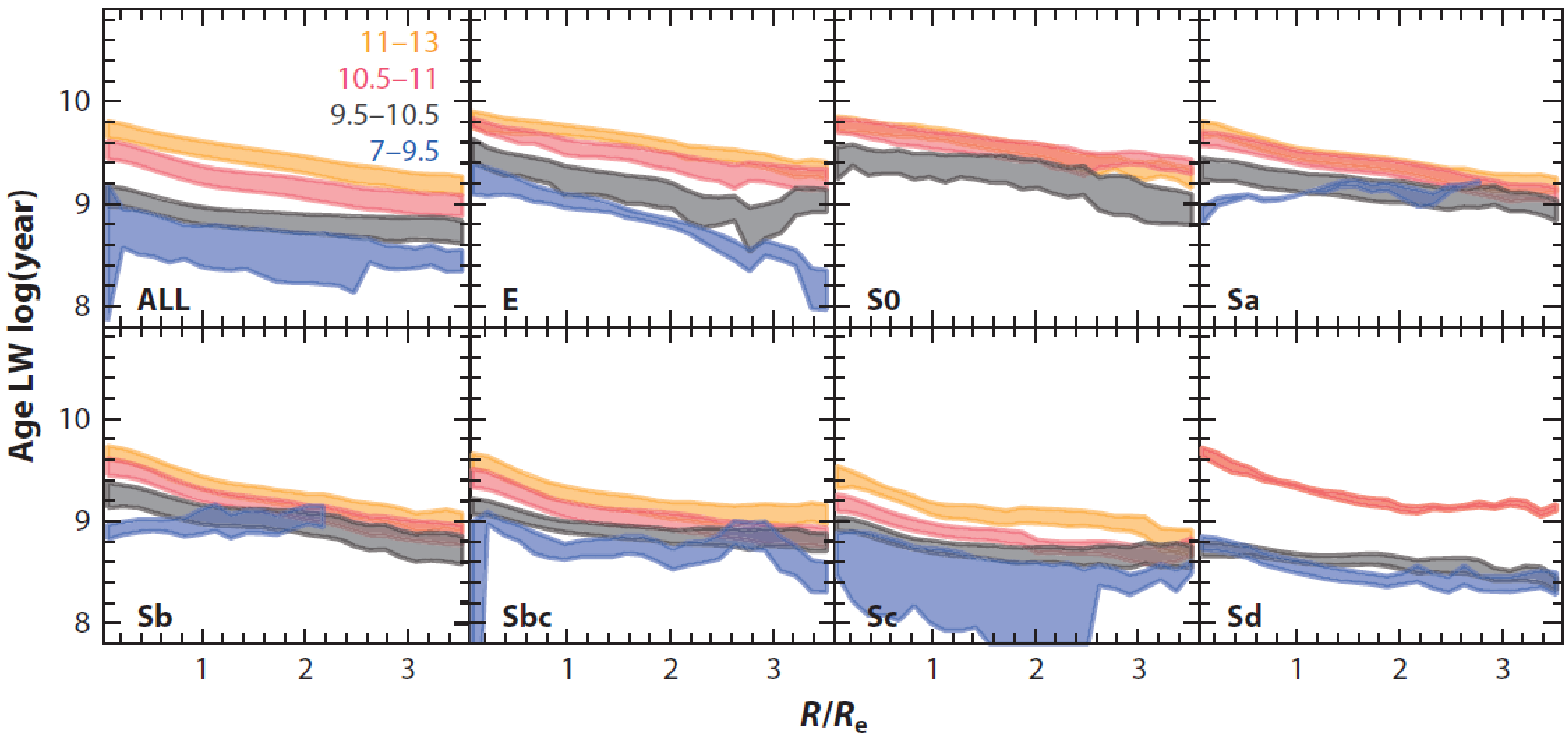

Figure 13

Azimuthally averaged radial distributions of the LW stellar ages for the galaxies in this review, segregated by stellar mass and morphology; colors and symbols have the same meanings as those in **Figure 12**. Abbreviation: LW, luminosity-weighted.

Sánchez ARAA 2020: compilation sample of 8177 z<0.06 nearby galaxies, the inner regions of galaxies more massive than $10^{9.5-10}$ Msun assemble their mass faster than the outer regions, following an inside-out growth (also Barden et al. 2005, van Dokkum et al.2013).

Cold Gas in galaxies

Atomic HI gas observed via the 21cm line at radio wavelengths. It is an important phase because gaseous disks extend beyond stellar orbits and allow us to measure dynamical masses and, also it is the reservoir to form molecular gas.

$$\frac{M_{HI}}{M_\odot} \simeq 2.36 \times 10^5 \left(\frac{D}{Mpc}\right)^2 \int \left[\frac{S(\nu)}{Jy}\right] \left(\frac{d\nu}{kms^{-1}}\right)$$

(Condon 2016 NRAO course online)

(1 Jy=10^{-26} W m^{-2} Hz^{-1})

E/S0s very little HI: e.g. only 9/389 ETGs in Virgo cluster detected by ALFALFA survey (Serego Aliguieri+ 2007), for dE M<3.5 x 10^7 $M_\odot$, for E/S0 M < 7.6 x 10^7 $M_\odot$ but higher detection rates in lower density environments (Grossi et al. 2009). THINGS survey (Walter et al. 2008) of 34 nearby galaxies, 2<D<15Mpc, early types excluded, measured HI gas masses:

range from

10^7 $M_\odot$ (dwarf S and Irr) to

10^{10} $M_\odot$ (giant S)

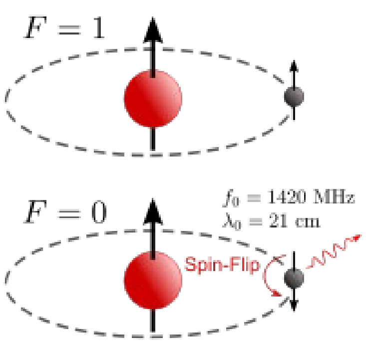

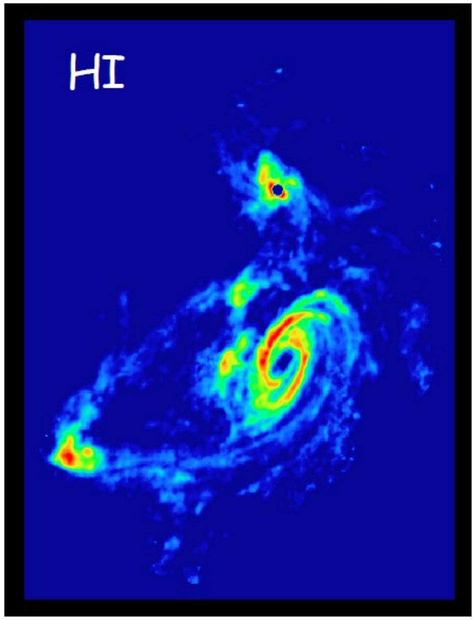

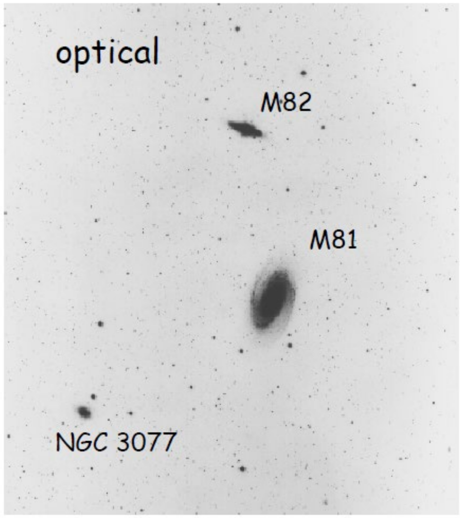

Cold Gas in galaxies

Molecular gas, dominated by H2, is most frequently inferred via CO transitions at mm-radio wavelengths. It is an important phase because this is the reservoir from which stars form: from M_{H2}~10^6 $M_{\odot}$ for Irr to ~ 10^{10} $M_{\odot}$ for Sp (Young & Scoville 1991 ARAA).

In the NGLS survey: 155 galaxies 2<D<25Mpc (Wilson et al. 2012)

$M_{H2} \approx 17.8 \times (R_{31}/0.18)^{-1} L_{CO(3-2)}$ where $R_{31} = L_{CO(3-2)} / L_{CO(1-0)}$

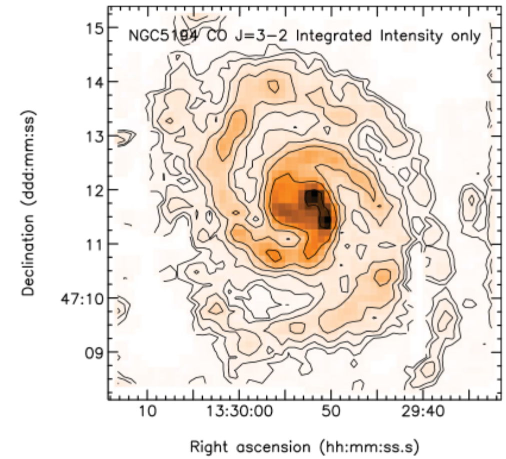

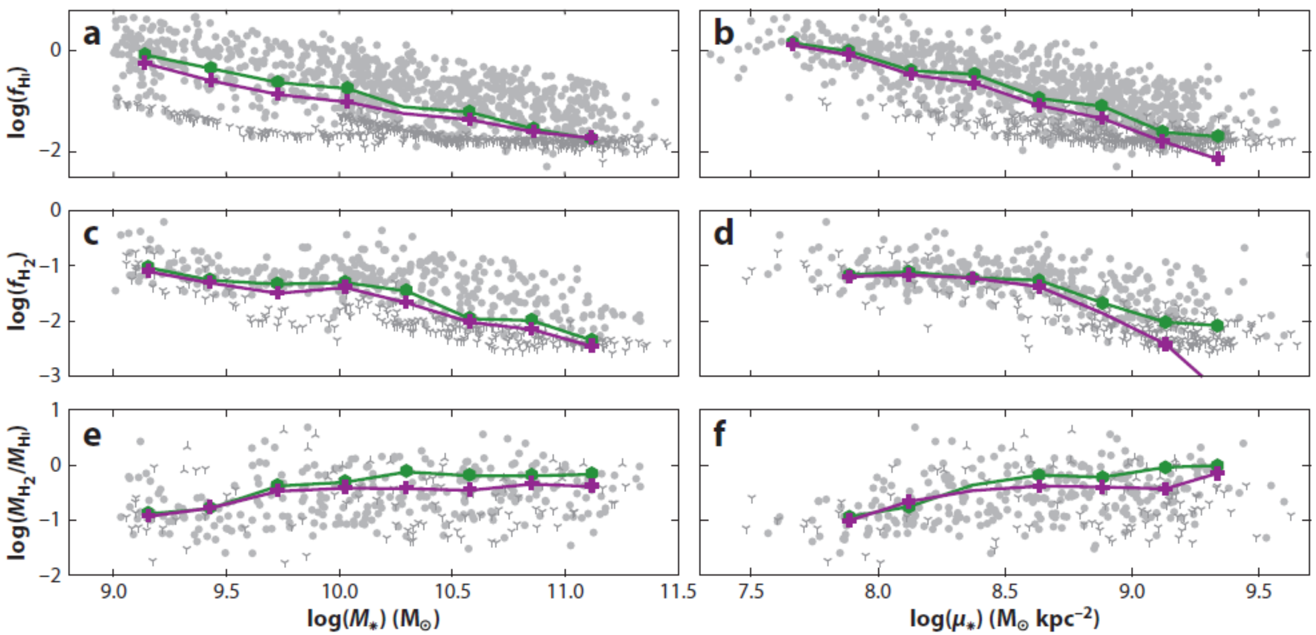

Overall at z~0 $M(H_2)/M(H)$~0.14 (Saintonge & Catinella 2023 ARAA).

Figure 4

Scaling relations between the atomic gas mass fraction ($f_{HI} \equiv M_{HI}/M_*$, *top row*), the molecular gas mass fraction ($f_{H_2} \equiv M_{H_2}/M_*$, *middle row*), and the molecular ratio (M_{H_2}/M_{HI}, *bottom row*) as a function of stellar mass (M_*, *first column*) and as a function of stellar mass surface density (μ_*, *second column*). The gray dots and Y-crosses are the xGASS and xCOLD GASS galaxies, and the binned values are calculated as medians (*green hexagons*) and mean values using survival analysis (*purple crosses*) as described in Section 4.1.

(Saintonge & Catinella 2023 ARAA).

Cold Gas in galaxies

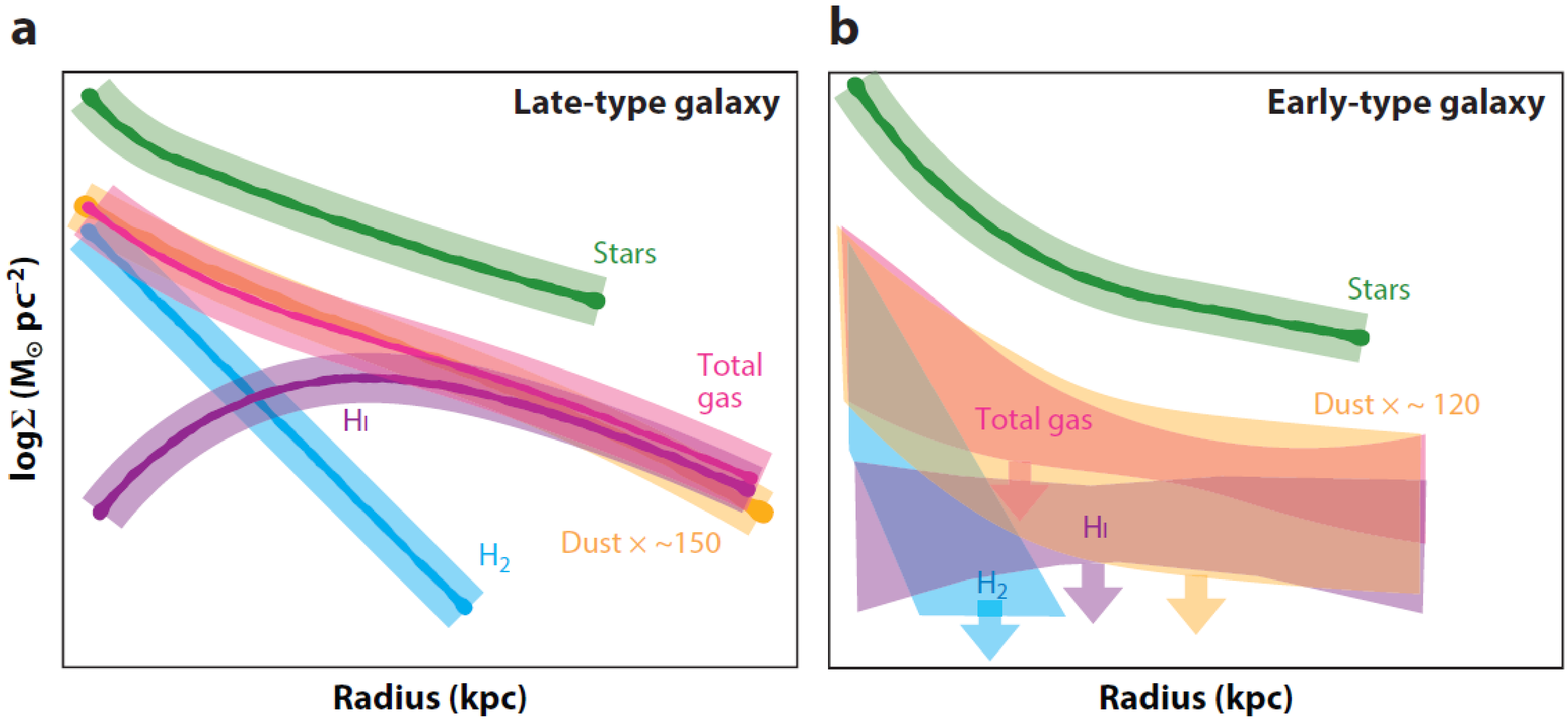

Figure 1

Radial distribution of cold gas, dust and stars in (*a*) a typical late-type galaxy and (*b*) a typical early-type galaxy of the nearby Universe. The spiral galaxy sketch is inspired by Casasola et al. (2017) and Bigiel & Blitz (2012). The elliptical model is based on ATLAS^{3D} and Herschel Reference Survey results (Serra et al. 2012, Smith et al. 2012, Davis et al. 2013). The dust curves have been scaled up by a typical gas-to-dust ratio for late- and early-type galaxies (De Looze et al. 2020, Smith et al. 2012).

(Saintonge & Catinella 2023 ARAA).

Warm ionized gas in galaxies

Warm ionized gas (T~few x1000 K), observed at UV-optical-IR wavelengths. Important since it is easily measured and it allows us to determine chemical abundances, kinematics of the Galaxy, and determine the sites and rates of recent star formation.

CALIFA: Integral Fiel Unit Spectroscopic survey of ~600 galaxies $0.005 < z < 0.03$ (D<130 Mpc)

(Sánchez+2012)

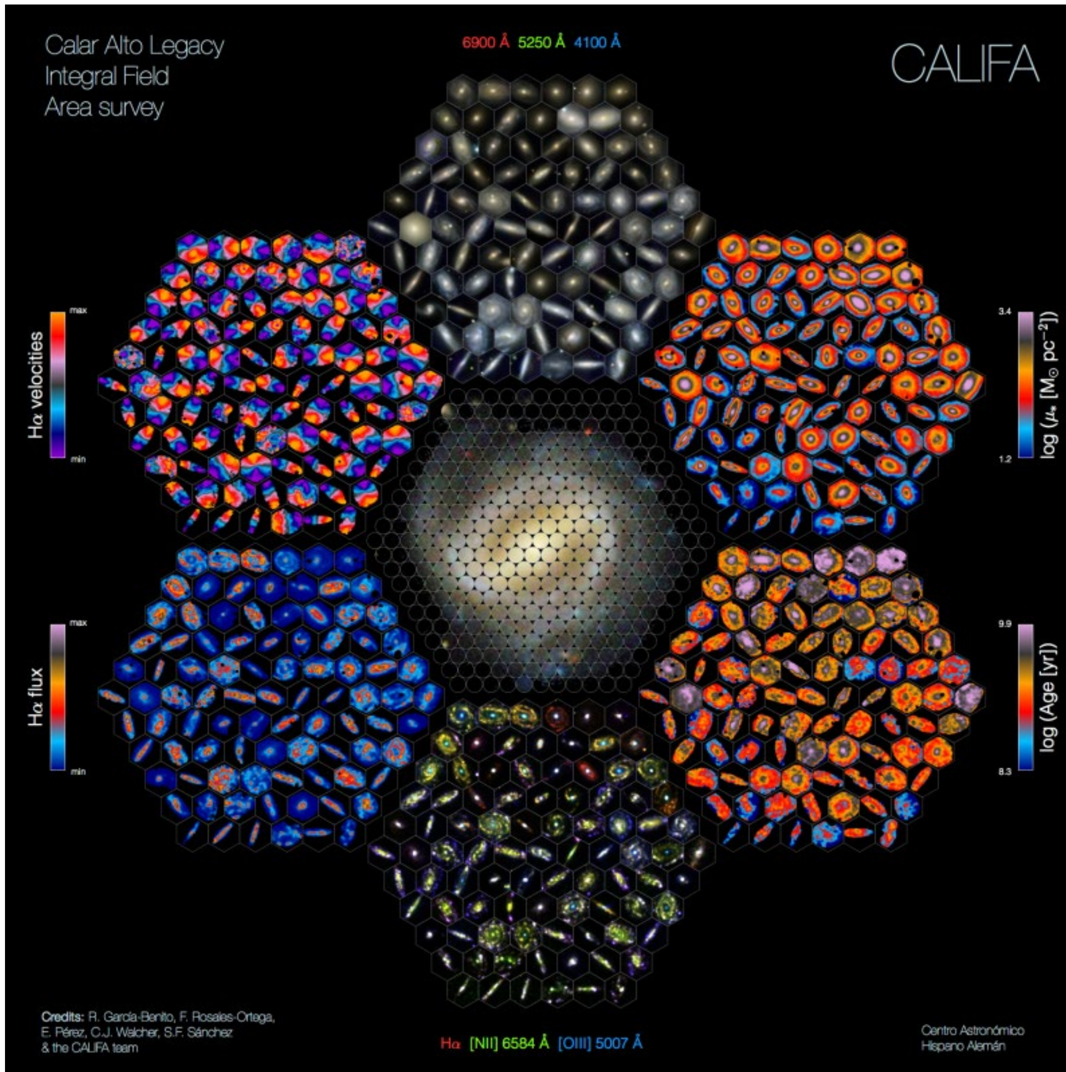

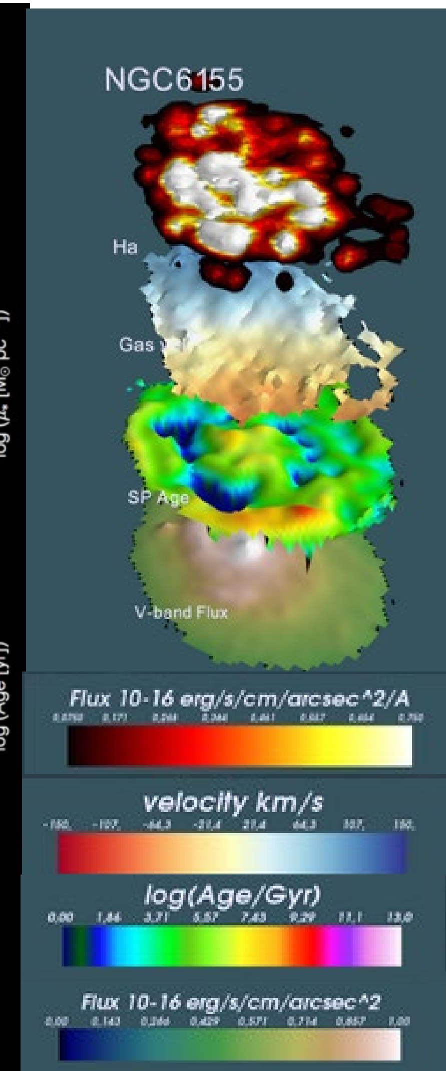

Warm ionized gas in galaxies

Warm ionized gas (T~few x1000 K), observed at UV-optical-IR wavelengths. Important since it is easily measured and it allows us to determine chemical abundances, kinematics of the Galaxy, and determine the sites and rates of recent star formation.

Reference for ionized gas determinations of density, temperature, chemical abundances etc: Osterbrock + Ferland Astrophysics of Gaseous Nebulae and Active Galactic Nuclei

Examples:

$$SFR(M_{\odot}/yr) = 7.9 \times 10^{-49} L_{H\alpha} (erg/s) \quad \text{(Kennicutt+ 1994)}$$

(http://www.caha.es/CALIFA/public_html/)

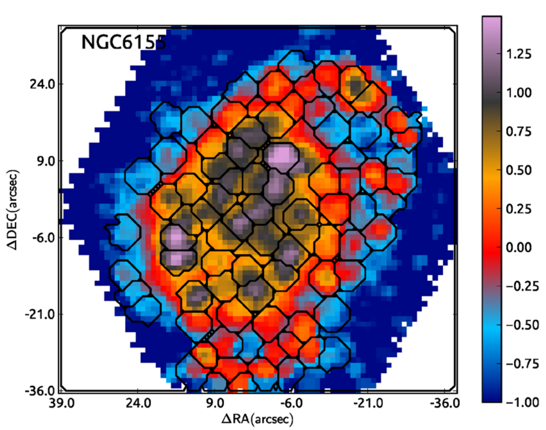

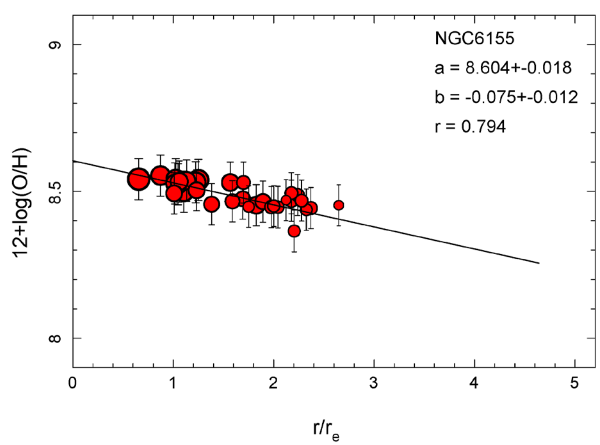

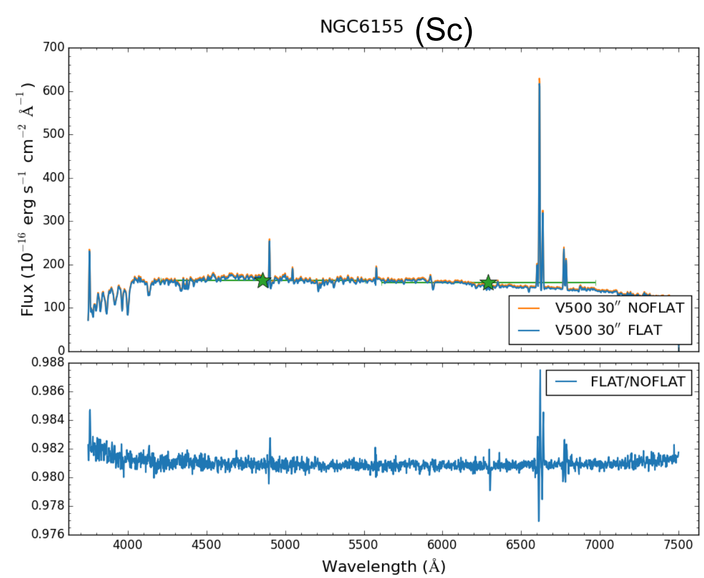

Dust in galaxies

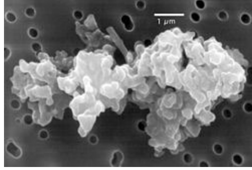

Dust are agregates of metals (elements heavier than He) ranging from a few molecules to ~0.1µm.

Dust is mixed with molecular gas, it absorbes the UV-optical radiation of stars and reemits it in the far- infrared-millimeter.

I. "lukewarm" component (T ~30-100 K): dust grains near to SF regions heated by young OB stars, which allows an indenpendent measurement of SFR
SFR: $SFR(FIR)(M_{\odot} yr^{-1}) = 1/\epsilon\ 4.5 \times 10^{-44} L_{FIR}(\mathrm{erg\ s^{-1}})$ (Kennicutt 1998)

I. cool (T~20 K) component by diffuse dust heated by general Interstellar Radiation Field

SLUGS survey of ~200 nearby galaxies at 450/850µm (Dunne+ 2000, Vlahakis+ 2005):

$M_d = \frac{S_{850} D^2}{k_{850} B(850\mu m\ T_d)}$ mass of dust, where S_{850} is the observed flux density, k_{850} is the dust opacity at 850um and B is the Planck function:

Mean dust masses Md~2 x $10^7 M_{\odot}$

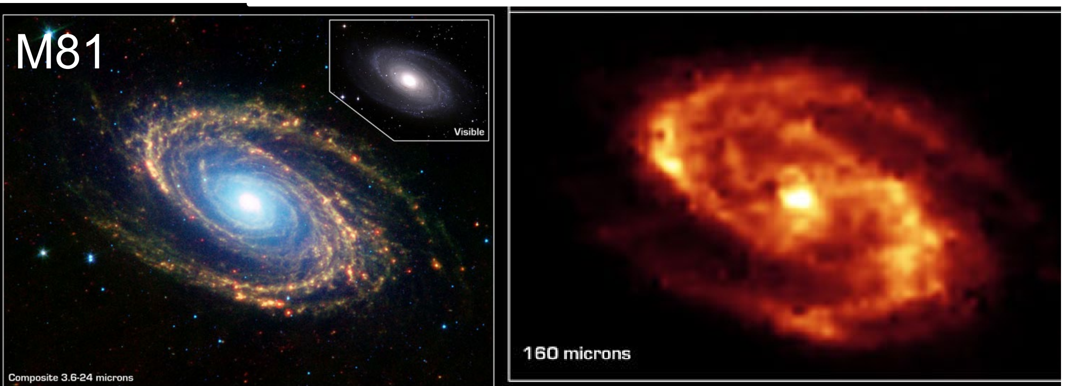

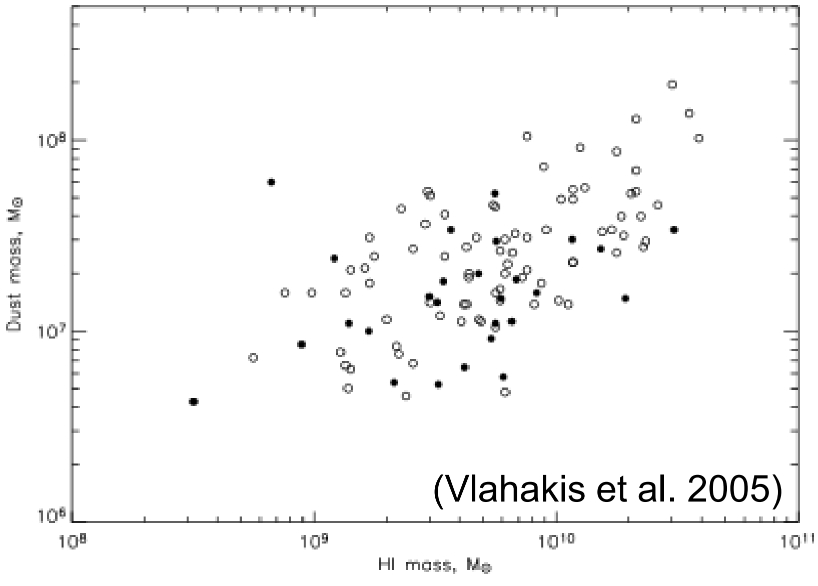

(Vlahakis et al. 2005)

Dust in galaxies: its effect on the SED

Dust is mixed with molecular gas, it absorbes the UV-optical radiation of stars and reemits it in the far- infrared-millimeter

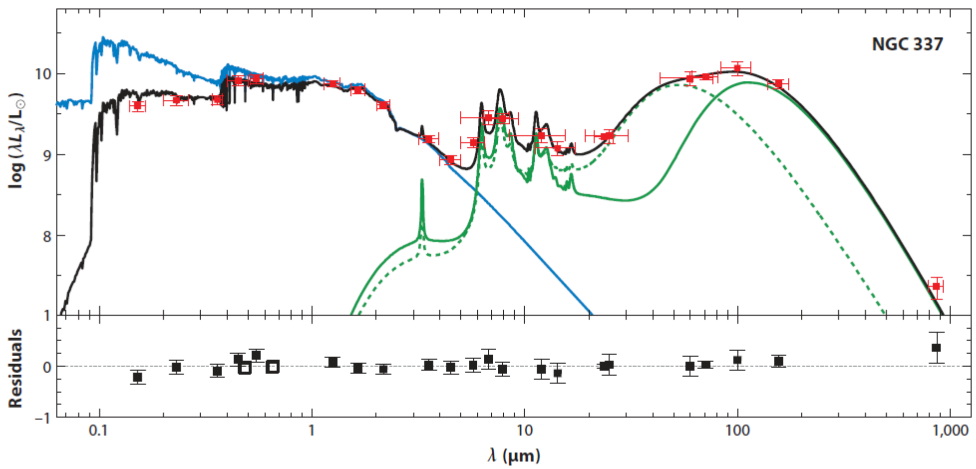

Popular screen extinction laws for UV-optical-IR: Milky Way, LMC, SMC, Starbursts (Calzetti), parametrized as $A(V) = R_V\ E(B-V)$ with *Rv*=3.1 (Cardelli et al. 1989)

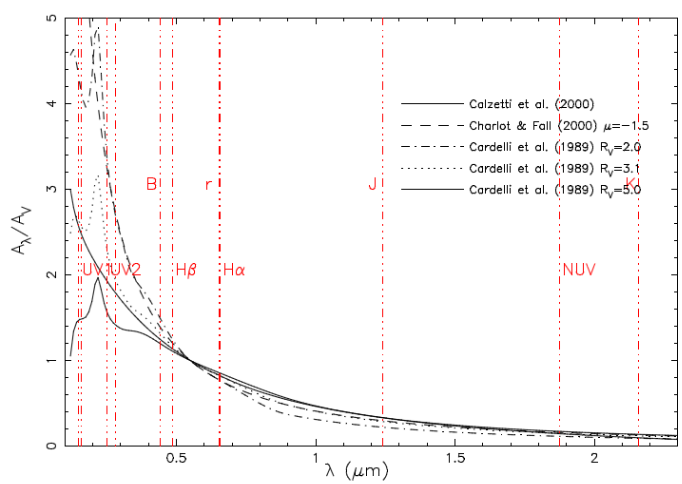

Evidence for DM in galaxies: rotational curves

If all the matter is concentrated near $r = 0$ where we see it:

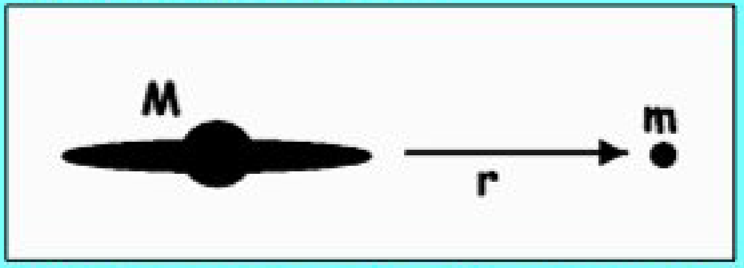

$$\frac{GMm}{r^2} = \frac{mv^2}{r}$$

$$v^2 = \frac{GM}{r}$$

$$\therefore v \propto r^{-\frac{1}{2}}$$

If the matter is distributed uniformly in a sphere with density ρ around the visible matter:

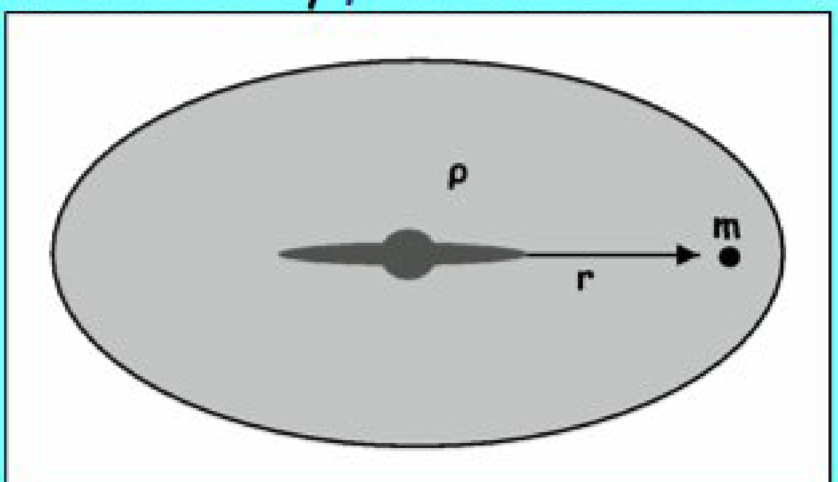

$$M = \frac{4}{3}\pi r^3 \rho \qquad v^2 = \frac{GM}{r}$$

$$v^2 = \frac{4}{3} G\pi r^2 \rho$$

$$\therefore v \propto r$$

Evidence for DM in galaxies: rotational curves

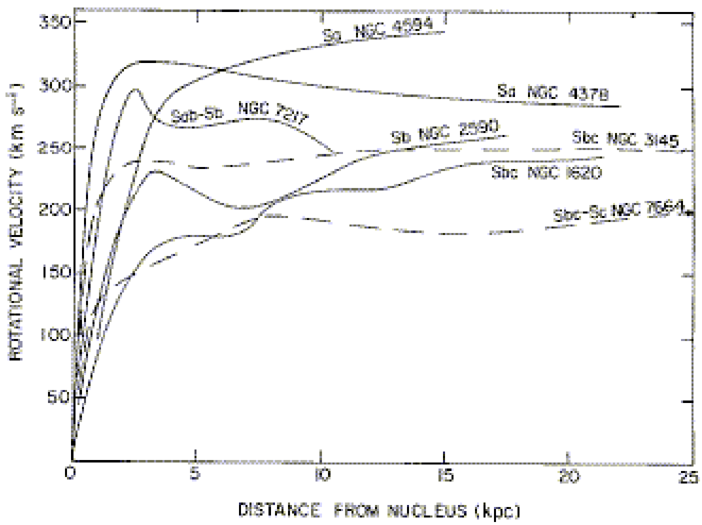

(Rubin et al. 1978)

FIG. 3.—Rotational velocities for seven galaxies, as a function of distance from nucleus. Curves have been smoothed to remove velocity undulations across arms and small differences between major-axis velocities on each side of nucleus. Early-type galaxies consistently have higher peak velocities than later types.

As Sofue & Rubin (2001, ARAA) recount: flat curves first detected through HI (Roberts & Rots 1973), and theoreticians predicted them (e.g. Ostriker & Peebles 1973) . Faber & Gallager (1979) reviewed why DM halos should be common around spiral galaxies.

In the most extreme cases the curve can be flat to ~100 kpc

M/L~10 $\pm$2 $M_\odot$ / $L_\odot$ inside 20 kpc .

M~$10^{14} M_\odot$ for Sp with v~250 km/s

Evidence for DM in galaxies: X-rays in E

Stellar kinematics can, in principle, be used, but complications due to anisotropies in orbits actually inhibits this method.

X-ray emission from $T \sim 5 \times 10^6$K (~10% of M_*), if in hydrodynamical equilibrium

$$\boxed{\frac{dP}{dr} = -\frac{GM\rho}{r^2} \Rightarrow M = \frac{k_B T r}{\mu m_p G}\left(-\frac{d\ln\rho}{d\ln r} - \frac{d\ln T}{d\ln r}\right)}$$

$M/L \sim 25 \pm 5\ M_\odot/L_\odot$ inside 20 kpc (Fabian et al. 1986).

$10^{12}\ M_\odot <\sim M_{vir} <\sim 10^{13} M_\odot$ for most Es (Buote & Humphrey 2011)

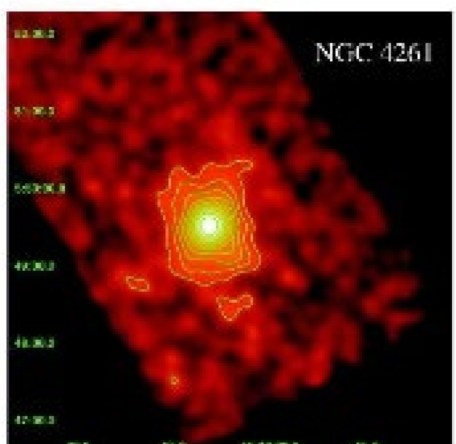

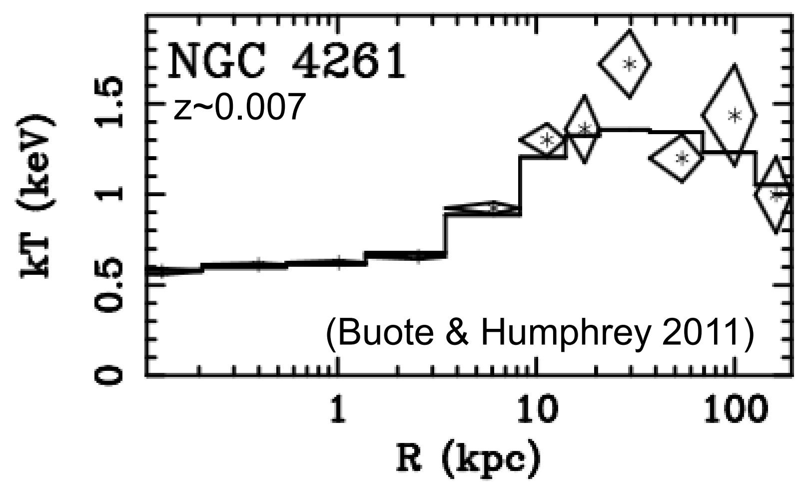

DM profiles in galaxies

Stellar to halo mass budget

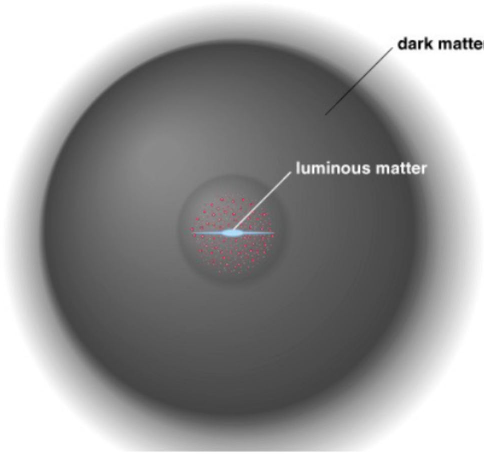

The mass in stars contained in each DM halo is a non-monotonic fraction of the halo mass.

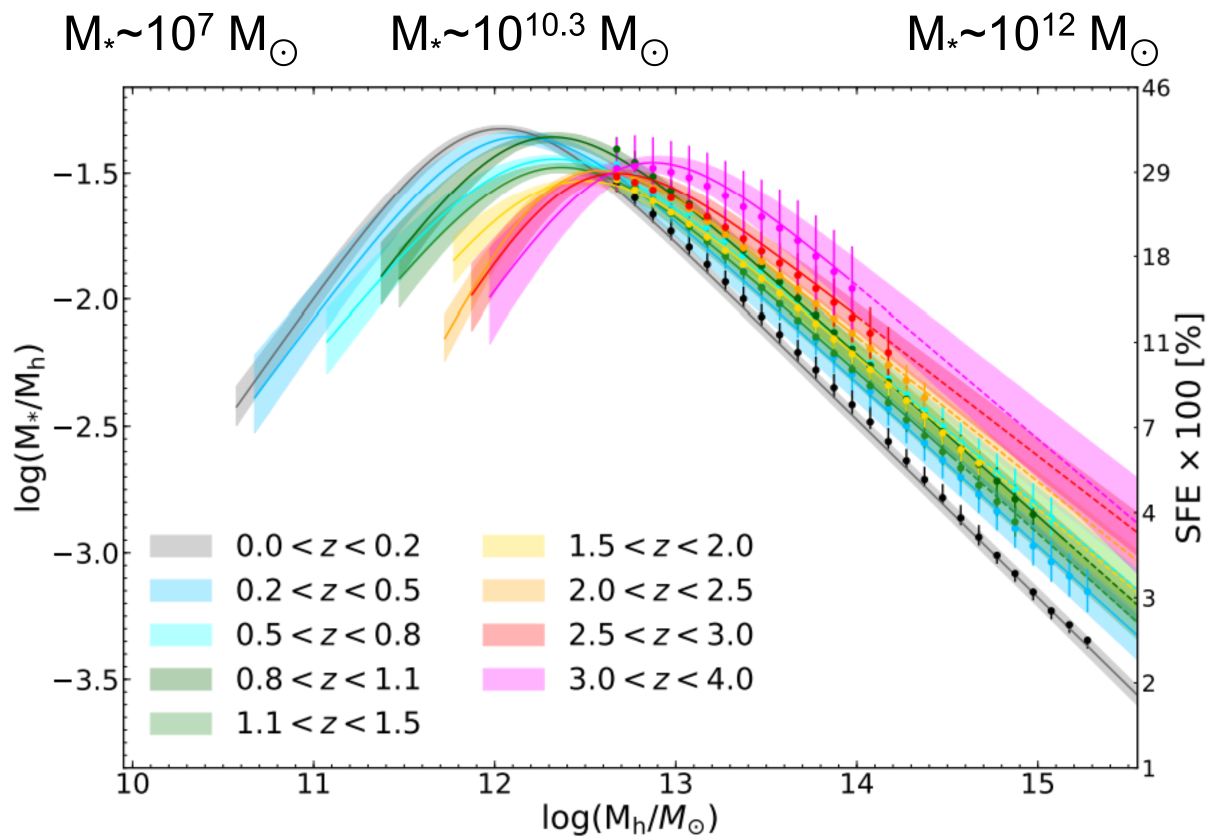

(Girelli et al. 2020)

Summary

E galaxies

Observable Evidence	***Implications***
red colours	*old stellar population*
high surface brightness	*densely packed stars*
smooth surface brightness profile	*relaxed system*
little evidence for dust	*gas resevoir depleted*
absorption line spectrum	*no current star formation*
little ordered rotation	*merger formation*
rare in field	*merger formation*

S galaxies

Observable Evidence	***Implications***
red colours in bulge	*old stellar population*
blue colours in disk	*younger stellar population*
moderate surface brightness	*relaxing*
moderate asymmetry	*relaxing*
significant amounts of dust	*gas resevoir present*
emission and absoprtion line spectrum	*current star formation and older population*
ordered rotation in disk	*formation via collapse*

Irr galaxies

Observable Evidence	***Implications***
blue colours	*young stellar population*
low surface brightness	*forming*
highly asymmetrical	*not a relaxed system*
significant amounts of dust	*gas resevoir present*
emission line spectrum	*current star formation*
ordered rotation	*formation via collapse*
common in field	*formation via collapse*

(from R. Guzmán´s viewgraph lib)

EXERCISE 1

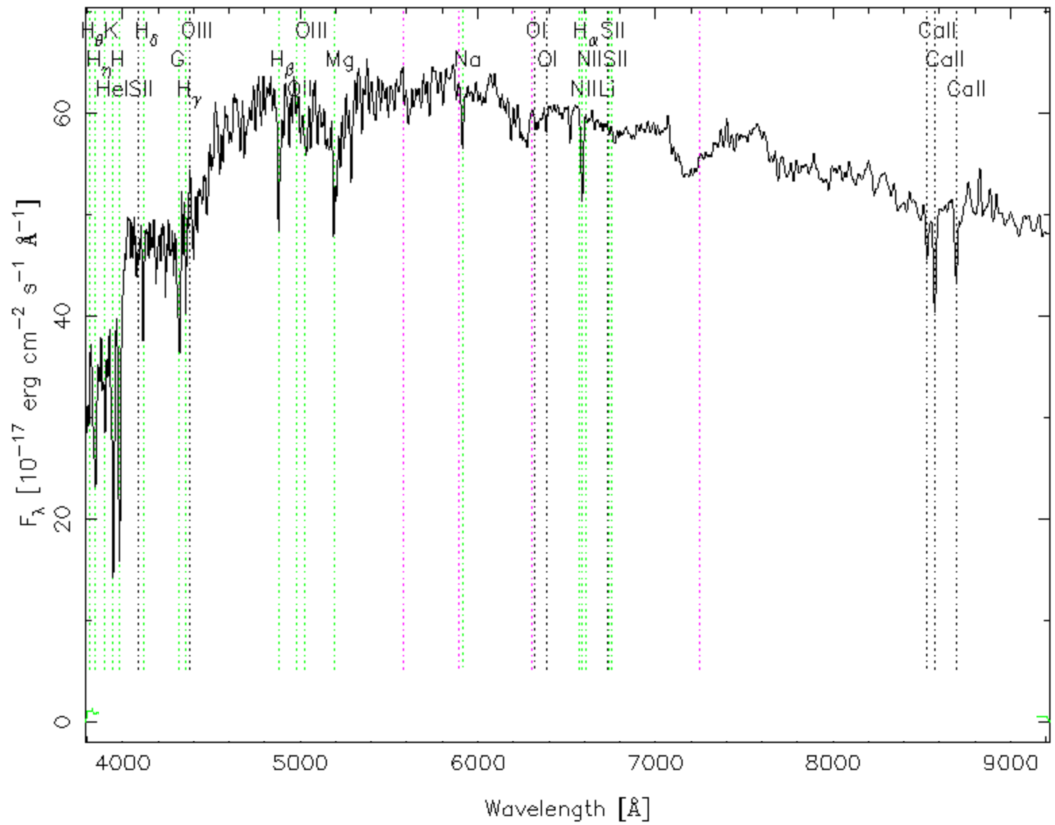

(SDSS)

Describe the spectrum of this galaxy. The Balmer line Hβ (rest frame 4861Å) is observed at 4877Å. What is the redshift of this galaxy? What is its “recession velocity”? What is its distance? If the object has an effective radius (which projected circle contains ½ total light) a 30” diameter in the sky, what is its projected physical diameter in kpc?

EXERCISE 2

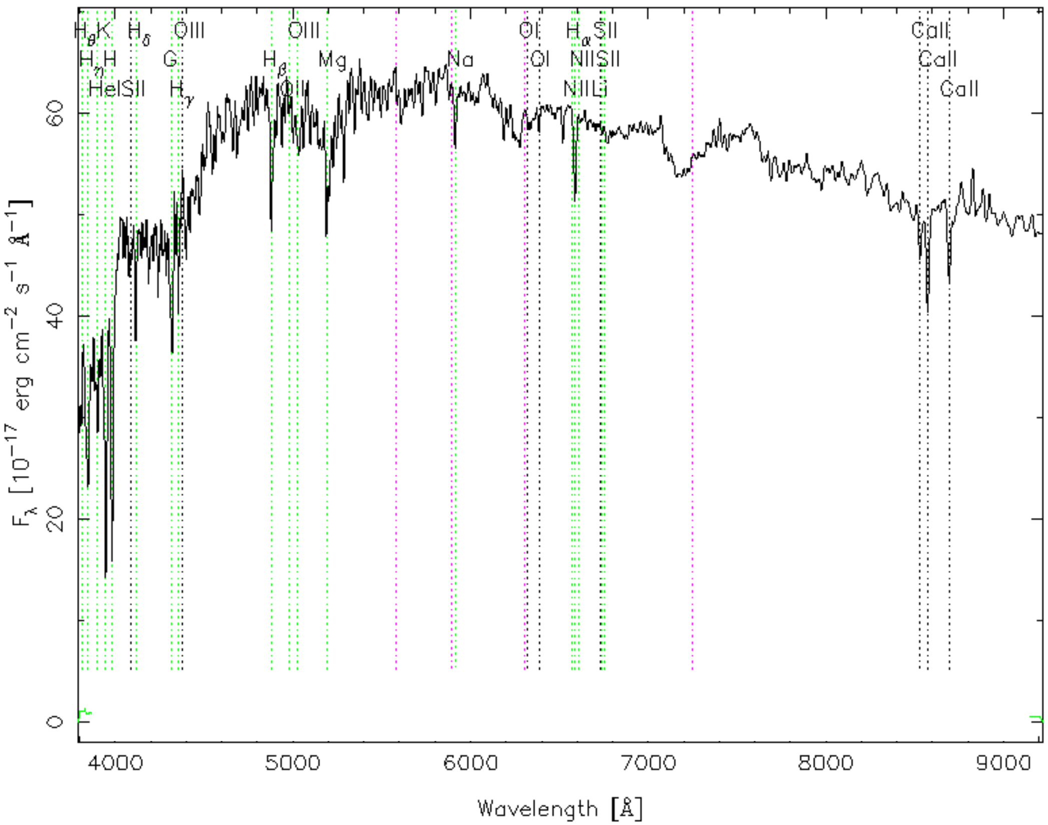

(SDSS)

Describe the spectrum of this galaxy (i.e., what information we may infer from the absorption lines and the lack of emission lines?). The Balmer line Hβ (rest frame 4861Å) is observed at 4877Å. What is the redshift of this galaxy? What is its distance? If the FWHM of the absorption line is 3.56Å. What is the velocity dispersion (σ) of this galaxy?

Galaxies

Itziar Aretxaga (itziar@inaoep.mx)
45 ISYA, Algeria, September 2024

Lecture 1: Introduction to the galaxy zoo:

- Galaxy types and classification schemes
- General properties and structure
- Standard stellar population indicators
- Dark matter in galaxies

Bibliography and important references:

• Ned Wright´s Cosmology Calculator:
http://www.astro.ucla.edu/~wright/CosmoCalc.html

• NASA Extragalactic Database: http://ned.ipac.caltech.edu

• Extragalactic Astronomy and Cosmology (2015), Peter Schneider, Springer.

• Mo, van den Bosch & White (2010). Galaxy Formation and Evolution, CUP.

• Galaxies in the Universe, Sparke & Gallagger, (2007), Cambridge University Press

(Acknowledgements to Pablo Pérez González and Rafael Guzmán for their lecture notes)